Plasma proteome fingerprint in kidney diseases

Kirill S. Nikolsky[1], Arthur T. Kopylov[1], Valeriya I. Nakhod[1],
Natalia V. Potoldykova[2], Dmitry V. Enikeev[2], Tatiana V. Butkova[1],
Liudmila I. Kulikova[1], Kristina A. Malsagova[1],
Vladimir R. Rudnev[1], Denis V. Petrovskiy[1], Alexander A. Izotov[1]
and Anna L. Kaysheva[1]*

[1]Laboratory of Structural Proteomics, Institute of Biomedical Chemistry, Moscow, Russia, [2]Institute for
Urology and Reproductive Health, I.M. Sechenov First Moscow State Medical University (Sechenov
University), Moscow, Russia

Introduction: Kidney diseases pose a serious healthcare problem because of their high prevalence, worsening of patients' quality of life, and high mortality. Patients with kidney diseases are often asymptomatic until disease progression starts. Expensive renal replacement therapy options, such as dialysis or kidney transplant, are required for end-stage kidney disease. Early diagnosis of kidney pathology is crucial for slowing down or curbing further damage. This study aimed to analyze the features of the protein composition of blood plasma in patients with the most common kidney pathologies: kidney calculus, kidney cyst, and kidney cancer.

Methods: The study involved 75 subjects. Proteins associated with kidney pathologies (CFB, SERPINA3, HPX, HRG, SERPING1, HBB, ORM2, and CP) were proposed. These proteins are important participants of complement and coagulation cascade activation and lipid metabolism.

Results: The revealed phosphorylated proteoforms (CFB, C4A/C4B, F2, APOB, TTR, and NRAP) were identified. For them, modification sites were mapped on 3D protein models, and the potential role in formation of complexes with native partner proteins was assessed.

Discussion: The study demonstrates that the selected kidney pathologies have a similar proteomic profile, and patients can be classified into kidney pathology groups with an accuracy of (70−80)%.

KEYWORDS

kidney diseases, kidney calculus, kidney cyst, cancer, tandem mass spectrometry, protein analysis, phosphorylation, candidate markers

1 Introduction

Understanding the molecular foundations of disease development opens up new opportunities for designing novel diagnostic approaches as well as searching for candidate biomarkers and protein drug targets. The pathogenesis of multifactorial diseases is determined by changes in gene expression and, therefore, changes in the protein profile of biospecimens as well as the presence of modified (aberrant) proteoforms (Kopylov et al., 2023; Tikhonov et al., 2021; Nikolsky et al., 2023). Comparative case–control studies fail to provide insight into whether there are any differences between

etiologically similar disease groups or determine specificity of the revealed candidate markers for segmentation of diseases of a certain organ. Implementation of research findings into medical practice is significantly impeded by low specificity of candidate biomarkers. In this context, conducting system research that focuses on the features of molecular profiles of etiologically similar diseases or diseases of one organ or tissue is rather relevant.

Our study addresses the most widespread kidney diseases. The comparison groups involved patients with kidney calculus, kidney cyst, and malignant kidney neoplasm. These pathologies are extremely common nowadays: up to 15% of global population are prone to the development of kidney calculus (Moftakhar et al., 2022) and at least 25%, simple kidney cysts (Garfield and Leslie, 2024). The annual incidence of kidney cancer is 400,000 new cases (Cirillo et al., 2024). There is heterogeneity in global epidemiology of these diseases: their highest prevalence is typical of Europe and North America.

These diseases have a largely similar clinical presentation (Table 1), thus hampering timely and accurate clinical diagnosis. Malignant transformation of kidney cysts (Tseng, 2015; Lu et al., 2021; Lai et al., 2019) and disease mimicry [e.g., renal cell carcinoma mimics kidney cyst (Jiang et al., 2015; Yu et al., 2017)] are possible.

Symptoms, clinical presentation, risk factors and even candidate molecular factors are often similar for kidney pathologies. Today, searching for markers or an ensemble of markers that would meet the clinical requirements for specificity, accuracy and sensitivity in the context of early diagnosis of kidney diseases is still ongoing. Thus, blood biochemistry test is recommended for suspected kidney cancer, with special attention paid to albumin blood level, the erythrocyte sedimentation rate, lactate dehydrogenase (LDH) and alkaline phosphatase activities, as well as blood levels of ionized and total calcium. These serologic factors are not specific to oncopathology (Table 1) but may affect the choice of treatment approach, as well as diagnostic and secondary prophylaxis options (Chen et al., 2017).

Elevated levels of reactive oxygen species, lipid peroxidation products, proinflammatory cytokines, and proangiogenic factors are typically detected in patients with kidney calculus (Wigner et al., 2021). Parameters recommended to be measured in these patients include the levels of cations (calcium, potassium, and sodium), C-reactive protein, creatinine, and albumin (EAU, 2024b; Vitale et al., 2008).

In patients with kidney cyst, blood chemistry parameters often remain normal if the cyst neither exerts pressure on adjacent tissue nor disturbs the renal function. For this disease, there are very few publications addressing the biochemical markers in blood of patients diagnosed with kidney cyst.

A proteomic analysis of blood samples collected from patients with verified diagnosis of kidney calculus, kidney cyst, or kidney cancer was conducted to identify proteins making the greatest contribution to segmentation of comparison groups. Phosphorylated proteoforms specific to groups of patients with kidney diseases were analyzed, and potential signaling pathways for pathology development were identified.

2 Materials and methods

2.1 Ethical consideration

Patients and healthy volunteers provided written consent to participate in the study, which was approved by the Local Ethics Committee of the Sechenov University (protocol No. 10–19 dated 17 July 2019). All handlings and use of material were provided according to the WMA Declaration of Helsinki on Ethical Principles for Medical Research Involving Human Subjects (the revision approved in Fortaleza, 2013). All the participants were aware of the research purpose. Informed consent was obtained from all the participants.

2.2 Participants

The study involved 75 subjects, including 51 patients having a verified diagnosis of a urologic disease: kidney calculus, kidney cyst, and kidney cancer, as well as 24 conditionally healthy subjects (control group). The inclusion criteria for the group of participants diagnosed with a urological disease were as follows:

– patient's age ≥18 years;
– ICD 10 code of the underlying disease: N20.0 "Calculus of kidney", N28.1 "Cyst of kidney, acquired", C64 "Malignant neoplasm of kidney, except renal pelvis".

The non-inclusion criteria were as follows:

– patients diagnosed with cancer of other organs and systems;
– psychoactive substance and alcohol abuse;
– pregnant or breastfeeding women.

The kidney disease (KD) group consisted of patients having kidney calculus and kidney cyst. The final diagnosis in the kidney cancer group (KC) was made based on multislice computed tomography (MSCT) and histologic examination.

Triple-phase helical computed tomography of the abdomen and the peritoneal cavity (kidneys) using the bolus-tracking technique was conducted regardless of disease stage in order to differentiate between benign and malignant tumors. Scans were acquired before and after administration of a contrast agent to assess its accumulation. Contrast enhancement of the neoplasm was determined by comparing the Hounsfield scale parameters (in Hounsfield units, HU) before and after administration of the contrast agent. Changes in contrast by at least 15 HU were regarded as contrast enhancement and viewed as a functionally active tumor region (EAU, 2024a). Malignancy and tumor grade were verified by postoperative histological examination.

Cystic structures were detected and classified using the Bosniak system. The group of patients with kidney disease comprised patients with Bosniak I or II cysts as these cystic structures are benign.

The number of subjects in the kidney disease (KD) group was 25; in the kidney cancer (KC) group, 26; and in the healthy (CNTR) group, 24 (Table 2). The comparison groups were matched with respect to the number of subjects and their age, sex, and height

TABLE 1 Comparison of clinical presentation of the development of kidney pathology.

Parameter	Kidney calculus	Kidney cyst	Kidney cancer
Disease and risk factor control			
Symptoms	• severe pain on either side of lower back • pain or stomach ache • hematuria • nausea or vomiting • fever and chills	• pain in the side, stomach or low back • hematuria • fever • changes in urination habits	• pain or dull ache in the side or lower back • hematuria • fever • changes in urination habits • rapid, unexplained weight loss
Diagnosis	Ultrasound computed tomography (USCT) or urography	Computed tomography (CT) Magnetic resonance imaging (MRI) Contrast-enhanced ultrasound (CEUS)	USCT or contrast-enhanced MRI; Histological diagnosis
BMI	Overweight (Moftakhar et al., 2022)	n/d	Obesity (Gray and Harris, 2019)
Diabetes mellitus	Yes (Moftakhar et al., 2022)	Yes (Wei et al., 2020)	Yes (Tseng, 2015)
Hematuria	Yes (Nagendra et al., 2023)	Yes (Boo et al., 2022)	No (Takeuchi et al., 2021)
Hypertension	Yes (Moftakhar et al., 2022)	Yes (Kim et al., 2014)	Yes (Gray and Harris, 2019)
Cigarette smoking	Yes (Moftakhar et al., 2022)	Yes (Sousa et al., 2021)	Yes (Gray and Harris, 2019)
Adults aged >40 years	Yes (Moftakhar et al., 2022)	Yes (Wei et al., 2020)	Yes (Tseng, 2015)
Sex	Yes	n/d	Yes (Ferlay et al., 2018; Moch et al., 2016)
Hereditary predisposition	Yes (Howles and Thakker, 2020; Singh et al., 2022)	Yes (Satariano et al., 2024; Park et al., 2021; Dillman et al., 2017)	Yes (Truong et al., 2022; Shuch and Zhang, 2018; Bratslavsky et al., 2021; Yanus et al., 2024)
Molecular factors			
Creatinine (serum)	Elevated (Katwal et al., 2022; Shastri et al., 2023; Shen et al., 2022; Pan et al., 2024)	n/d	Elevated (Liu et al., 2020; Zhang and Bu, 2022)
Urea (serum)	Elevated (Katwal et al., 2022)	n/d	Elevated (Sun et al., 2021; Bai et al., 2021; Li et al., 2019)
Uric acid (serum)	Elevated (Kc and Leslie, 2024; Tung et al., 2024; Alelign and Petros, 2018)	Elevated (Abbiss et al., 2019)	Elevated (Allegrini et al., 2022; Dai et al., 2020)
Calcium (ionized or total)	Elevated (Alelign and Petros, 2018)	Elevated (Mangolini et al., 2016)	Hyperelevated (Vakiti et al., 2024)
Albuminuria	Elevated (Alelign and Petros, 2018; Brewin et al., 2021)	Elevated (Boo et al., 2022)	Elevated (Luo et al., 2023a; Luo et al., 2023b; Mok et al., 2020)
C-reactive protein	Elevated (Shoag and Eisner, 2014)	Elevated (Bergmann et al., 2018)	Elevated (Zhou et al., 2015)
Lactate dehydrogenase (LDH)	Elevated (Devi et al., 2023; Ding et al., 2021; Xiao et al., 2023)	n/d	Elevated (Claps et al., 2022; Wu et al., 2021; Mishra and Banerjee, 2019)
Interleukin-1 (IL-1)	Association (Xiao et al., 2022)	Association (Yang et al., 2019)	Association (Sindhughosa and Pranamartha, 2017)
PKD1/PKD2	n/d	Association (Yang et al., 2023; Al-Hamed et al., 2019)	Association (Meguro et al., 2023)
Alkaline phosphatase	Elevated (Palsson et al., 2019; Zhu et al., 2023)	n/d	Elevated (Stebbing et al., 2014; Stanford and Bottini, 2023)

TABLE 2 Anthropometric characteristics of the study participants.

Parameter	Kidney disease (KD)		Kidney cancer (KC)		Healthy group (CNTR)	
ICD-10 code of the underlying disease	N20.0 "Calculus of kidney"; N28.1 "Cyst of kidney, acquired"		C64 "Malignant neoplasm of kidney, except renal pelvis"		–	–
Sex	female	male	female	male	female	male
Number of participants (n)	15	10	11	15	12	12
Age (years)	59 ± 11.83 ($p = 0.47$)	58.5 ± 13.74 ($p = 0.6$)	57 ± 7.88 ($p = 0.72$)	60 ± 5.47 ($p = 0.6$)	60.5 ± 3.7	59.5 ± 2.19
Weight (kg)	76 ± 12.85 ($p = 0.05$)	86.5 ± 12.73 ($p = 0.001$)	98 ± 12.37^a ($p = 0.002$)	95 ± 9.97^a ($p = 0.0003$)	68.5 ± 5.92	68.5 ± 7.35
Height (cm)	164 ± 7.17 ($p = 0.32$)	179.5 ± 4.84 ($p = 0.05$)	164 ± 3.03^a ($p = 0.38$)	182 ± 6.88^a ($p = 0.05$)	171.5 ± 9.21	173.5 ± 6.89
BMI (kg/m^2)	28.3 ± 5.18 ($p = 0.01$)	25.43 ± 3.86 ($p = 0.001$)	35.9 ± 4.72^a ($p = 0.001$)	27.8 ± 3.65^a ($p = 0.0002$)	23.51 ± 1.57	22.89 ± 1.66

[a]– according to the available data; p-value (Benjamini–Hochberg adjusted) are provided with respect to the values of the control (comparison) group of patients of the respective sex.

distribution. Differences in these parameters between comparison groups were non-significant among males and females ($p \geqslant 0.05$).

The body mass index (BMI) parameters come under notice, which differed significantly in the KD and KC groups compared to patients in the control group. The mean BMI among all the female urologic patients was 32.1 ± 4.95 kg/m^2, which corresponded to overweight or class 1 obesity. Among male patients, this parameter was 26.62 ± 3.76 kg/m^2, mostly corresponding to normal body weight or overweight. Patients diagnosed with kidney cyst or kidney calculus had BMI = 28.3 ± 5.18 kg/m^2 (females) and 25.43 ± 3.86 kg/m^2 (males). For study subjects diagnosed with kidney cancer, BMI was 35.9 ± 4.72 kg/m^2 among females (corresponding to class 1 and 2 obesity) and 27.8 ± 3.65 kg/m^2 among males (mostly overweight and class 1 obesity). The control group consisted of conditionally healthy subjects with BMI lying in the normal range.

2.3 Blood sample collection

Blood samples in study subjects were collected strictly after fasting, at 8.00–10.00 a.m., in a clinical diagnostic laboratory. For proteomic analysis, blood samples were collected from the cubital vein into vacutainer tubes containing 3.8% sodium citrate anticoagulant (Improvacuter, Guangzhou Improve Medical Instruments Co., Ltd., Guangzhou, China). The samples were centrifuged at 3,000 rpm during 6 min at room temperature. Each plasma sample (500 µL) was collected into two dry Eppendorf polypropylene microtubes, frozen, and stored at −80°C until analysis.

2.4 Blood chemistry test

Blood chemistry tests were conducted on a Torus 1,200 semi-automatic chemistry analyzer (Moscow, Russia). Reaction mixtures were prepared in accordance with the manufacturer's instructions. The measurements were performed using the kinetic method, the

endpoint method, and fixed time. Quality control was performed by measuring control "normal" (TruLab N) and "pathological" (TruLab P) sera (DiaSys Diagnostic Systems GmbH, Germany). The reference values from the application sheets are summarized in Table 3.

2.5 Preliminary preparation of blood plasma for HPLC-MS/MS analysis

Preliminary preparation of blood plasma for proteomic analysis was thoroughly described in Stepanov et al. (2023). The protein fraction was precipitated with methanol (JT Baker, Landsmeer, the Netherlands). Alkylation was performed in the presence of 2% 4-vinylpyridine solution (Aldrich, Gillingham, United Kingdom) in 30% isopropanol solution (Fisher Chemical, Laughborough, United Kingdom). Trypsinolysis (~400 ng trypsin per sample, Promega, Madison, Wisconsin, United States) involved two steps and was performed in 75 mM triethylammonium bicarbonate buffer (pH 8.2). The hydrolysates were vacuum dried before storage (Concentrator Plus, Eppendorf, Hamburg, Germany). Before mass spectroscopy measurements, the dry residue was re-dissolved using 0.1% formic acid (Acros Organics, Geel, Belgium).

2.6 Mass spectrometry analysis

Spectra were acquired on a Xevo™ G2-XS Q-TOF quadrupole time-of-flight mass spectrometer (Waters, Wilmslow, United Kingdom) in the positive ionization mode within a normal dynamic range of masses. The capillary voltage was 3 kV; the cone voltage was 67 V. The drying gas flow rate was 680 L/min; the focusing gas velocity was 50 L/min. The source temperature was set at 150°C; desolvation temperature was set at 350°C. Ions were surveyed in the data-independent acquisition mode (SONAR). The full MS scanning was performed in a range of 300–1,300 m/z with a low-energy CID fragmentation at 6 eV, followed by scanning in the SONAR mode with quadrupole mass start at m/z = 178 and quadrupole

TABLE 3 Blood chemistry parameters of venous blood and their reference values.

Parameter	Abbreviation	Reference values		Units
		Male	Female	
Alanine aminotransferase	ALT	10-40 (Eliseev, 2023)	7–35	U/L
Aspartate aminotransferase	AST	<40 (Eliseev, 2023)	<40	U/L
Alkaline phosphatase	ALP	<270 (Eliseev, 2023)	<240	U/L
Albumin	ALB	35–50		g/L
Triglycerides	TRIG	40–49 years 0.63–3.37 >50 years 0.70–3.25 (Eliseev, 2023)	40–49 years 0.50–2.10 >50 years 0.62–2.79	mmol/L
Creatinine	Cr	>60 years 71–115 (Eliseev, 2023)	>60 years 53–106	µmol/L
Glucose	Glu	>60 years 4.6–6.4		µmol/L

mass stop at m/z = 1,287 with a 22 Da mass window and high-energy CID fragmentation range from 15 to 37 eV. The total time for a complete scan cycle was set at 0.418 s. Mass correction using leucine–enkephalin (m/z = 556.2771, z = 1+) injected every 30 s at a concentration of 50 pg/mL was active at scanning times from 0.5 to 59 min.

Chromatographic separation was performed on an Acquity™ UPLC H-Class Plus chromatography system (Waters, United Kingdom) using a BEHC18 column (1.7 µm particle size, geometry 2.1 × 50 mm; Waters, United Kingdom) at 40°C and a flow rate of 0.3 mL/min in gradient mobile phases A (water) and B (acetonitrile) supplemented with 0.1% formic acid and 0.03% acetic acid. The following elution gradient was applied: 0–1.5 min, 3% B; up to 26.5 min, 19% B; up to 42 min, 32% B, and up to 43.5 min, 97% B; the column was then exposed to the isocratic mode up to 47.5 min and 3% B at 49 min. The post-run column equilibration lasted 6 min.

The obtained data were analyzed using the PLGS (Protein Lynx Global Server, version 3.0.3, Waters, United Kingdom) software employing the UniProt KB database with preset parameters for the SONAR/MS[E] scanning mode (Stepanov et al., 2023). The data were processed using the Apex 3D mode with a lock-mass correction of leucine–enkephalin (m/z = 556.2771[1+]) within 0.2 Da detection window. Low-energy and high-energy intensity thresholds were adjusted to 60 and 10 counts, respectively, between 0.5 and 49 min of the acquired data. Spectral data after processing were browsed against Uni Prot KB (release September 2023) protein sequences with a concatenated reverse-sequences database. Ions were surveyed with a peptide tolerance of ±25 ppm and fragment ion tolerance of ±75 ppm using at least three fragment ion matches per peptide and at least two peptide matches per protein after digestion with trypsin with a maximum of one missed cleavage. S-pyridylethylation was applied as a fixed type of modification, while S, T and Y phosphorylation (SEP, TPO and TPR) was applied as a variable modification. Peptide and protein identifications were percolated using the 2% false discovery rate. The mass spectrometry proteomics data have been deposited to the ProteomeXchange Consortium via the PRIDE (Perez-Riverol et al., 2021) partner repository with the dataset identifier PXD051799 "Kidney disease proteome research"

(Reviewer account details: Username: reviewer_pxd051799@ebi.ac.uk; Password: R858MIv3).

2.7 Data analysis

PSMs detected with PLGS were processed with two steps:

1. Filtering: only samples with more than 70 unique proteins (by UniProt ID) identified in sample were chosen for next steps;
2. Imputation: missing concentration values for PSMs were predicted using ordinary least squares (OLS) linear regression based on the available intensity values.

Differentially expressed proteins were identified for a sample (N = 57) filtered according to the following criteria:

1. Protein is found in ≥50% samples within a group;
2. Concentration was imputed in ≤50% protein samples within a group.

The fold change value was calculated as follows:
If $C_{ctrl} > C_{test}$, then $fCh = \frac{C_{test}}{C_{ctrl}}$; else $fCh = \frac{C_{ctrl}}{C_{test}}*(-1)$, where C_{cntr} is the median protein concentration in the control group; C_{test} is the median protein concentration in the comparison group; fCh is the fold change.

The p-value was determined by Mann–Whitney U rank test (Mann and Whitney, 1947) in the scipy. stats package (SciPy, 2024b). False discovery control was performed employing the Benjamini–Hochberg procedure (Benjamini and Hochberg, 1995) also using the scipy. stats package (SciPy, 2024a).

Principal component analysis (PCA) and Sparse partial least-squares discriminant analysis (sPLS-DA) with 0.95 ellipse confidence were conducted using the MixOmics software package for R programming language (mixOmics, 2024) based on the examples of using these methods (sPLSDA SRBCT Case Study, 2024; mixOmics Vignette, 2024) for a group of proteins (N = 104) that were identified in no less than 20 samples.

TABLE 4 Blood chemistry parameters of study subjects.

Parameter	Kidney disease (KD)[a]	Kidney cancer (KC)[a]	Healthy group (CNTR)[a]
Glu (µmol/L)	5.2 ± 1.96 ($p = 0.002$)	5.25 ± 1.29 ($p = 0.002$)	3.8 ± 1.39
TRIG (µmol/L)	1.16 ± 0.55 (p= 0.000001)	0.98 ± 1.72 ($p = 0.00003$)	0.32 ± 0.24
ALB (g/L)	36 ± 13.18 ($p = 0.86$)	35.5 ± 9.37 ($p = 0.86$)	35 ± 7.81
ALT (U/L)	9.5 ± 4.22	4.0 ± 4.3	n/d
AST (U/L)	10.05 ± 4.47	10.57 ± 3.44	n/d
ALP (U/L)	132.5 ± 29.85	171 ± 75.62	n/d
Cr (µmol/L)	67 ± 18.62	64 ± 16.9	n/d

[a]– according to the available data; p-value (Benjamini–Hochberg adjusted) are provided with respect to the values of the control (comparison) group of patients of the respective sex.

The acceptance criteria for protein identification were based on the Human Proteome Project Mass Spectrometry Data Interpretation Guidelines 3.0 (Malsagova et al., 2024): a candidate feature in the proteomic data had to meet the unicity criterion, meaning that certain proteins had to be covered by more than one unique protein-specific peptide without interference from any other protein.

3 Results

3.1 Analysis of blood chemistry data

In all study subjects, blood chemistry parameters were either normal or lay within the lower limit of the normal range. Slight decline in albumin level as well as reduced creatinine level and alanine aminotransferase activity were observed in the group of patients with kidney cancer. Blood glucose, triglyceride, and albumin levels were either normal or slightly decreased in the group of conditionally healthy subjects (Table 4).

For all thee selected parameters, the resulting values lie within the normal range. However, triglyceride and glucose levels in the KD and KC groups are significantly elevated compared to the CNTR group. The normal ranges of blood chemistry parameters in the KC group are possibly caused by the fact that in almost all the cases, there was a malignant tumor structure sized ≤7 cm, correlating with stage T1 according to the UICC TNM Classification of Malignant Tumors 2017, eighth edition (Brierley et al., 2017).

3.2 Plasma proteins

A total of 644 proteins were identified in the analyzed samples; 163 of them were shared among comparison groups (Figure 1A). Only few proteins were specific to groups of patients with kidney pathologies KC or KD. For this reason, no analysis of group-specific proteins was conducted.

The identified proteins shared by the analyzed comparison groups are expectedly involved in important biological processes (Figure 1B): classical antibody-mediated complement activation (R-HSA-173623, n = 46); FCGR activation (R-HSA-2029481, n = 45); binding and uptake of ligands by scavenger receptors (R-HSA-2173782, n = 54). A full list of shared proteins is provided in Supplementary Table S1.

Table 5 summarizes proteins whose blood level (fold change) differs for the selected comparison groups (KD and KC) with respect to control. The blood levels of proteins involved in immune response are simultaneously elevated in two comparison groups (kidney disease (KD) and kidney cancer (KC)) with respect to the control group. Thus, the blood level of complement factor B (P00751) in patients with kidney cancer increased 1.7-fold (p = 0.004); similar elevation was observed in patients in the kidney disease group (1.4-fold; $p = 0.13$). Furthermore, the blood levels of such proteins as alpha-1-acid glycoprotein 2 (P19652) (p = 0.02) and ceruloplasmin (P00450) (p = 0.04) in patients in the kidney disease and kidney cancer groups were also simultaneously increased 1.4-fold and 1.3-fold, respectively. The maximum change in protein level was observed for hemoglobin subunit beta (P68871): its level increased more than twofold ($p = 0.08$) in the KD group and more than fourfold, in the KC group (p = 0.0008).

The comparison groups could not be segmented by principal component analysis (PCA): the proteomic profiles were found to densely overlap (Figure 2A). For achieving discrimination, we performed selection and classification of descriptors using sparse partial least-squares discriminant analysis (sPLS-DA) (Figure 2B). The 12.5% and 15% variance in the consolidated proteome was interpreted by discriminant analysis (Figure 2B). Figure 2B demonstrates that the proteomic profiles corresponding to the control group differ to the maximum extent from the group of patients having a pathology. Meanwhile, the profiles of the KD and KC groups overlap as indicated by the large area of proteomic profile overlaps. Figure c shows that in general, the analysis provides a fair result of data segmentation into comparison groups (70%–80%).

In all three images in Figure 2A–C, the values referring to the control group, the KD group, and the KC group are shown in red, blue, and green, respectively. The absolute weights of the sparse loading vectors for each sPLS-DA dimension in the data set are presented in Supplementary Table S2; Figure 3 shows proteins with the greatest weights, including those whose level varied significantly.
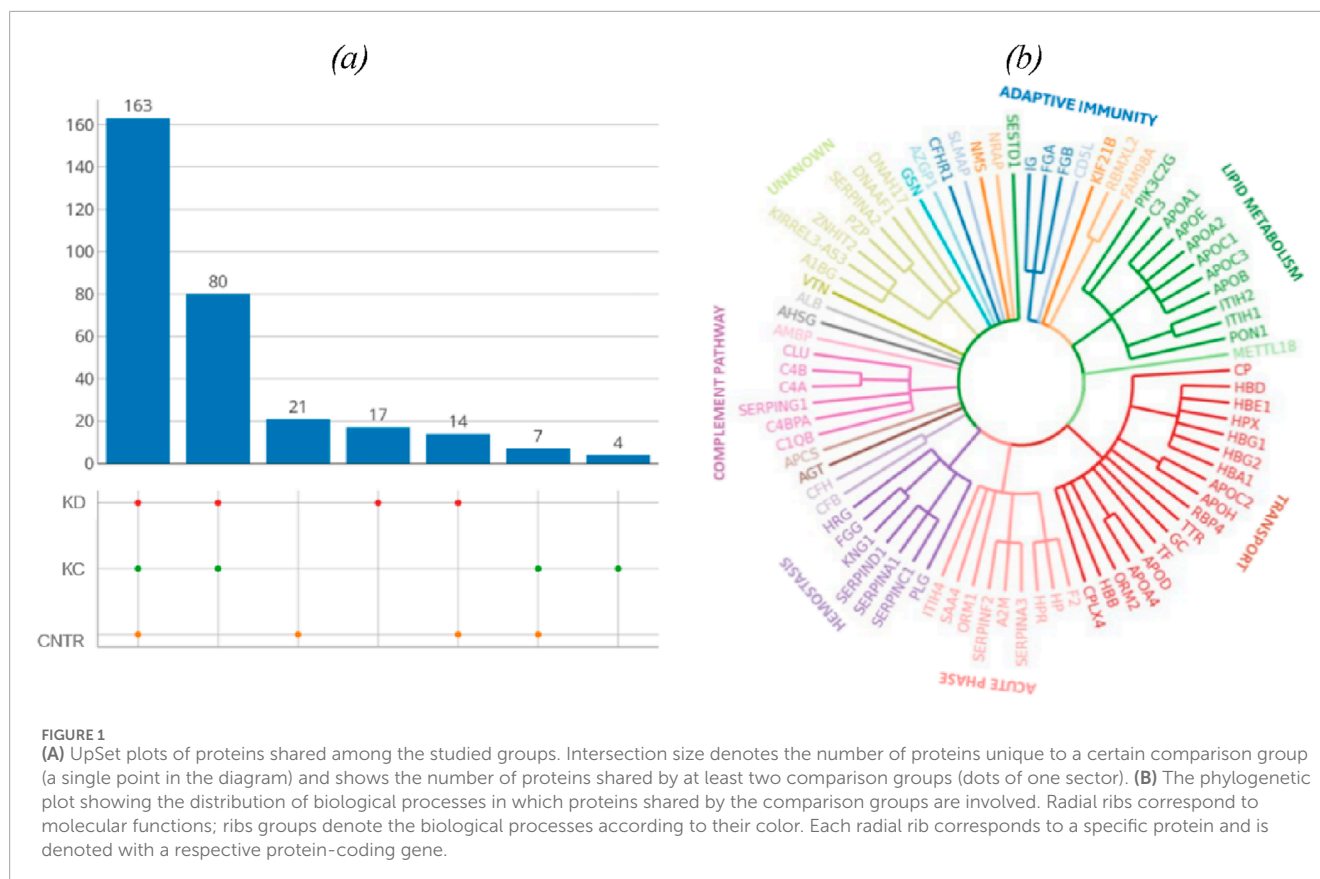
FIGURE 1
(A) UpSet plots of proteins shared among the studied groups. Intersection size denotes the number of proteins unique to a certain comparison group (a single point in the diagram) and shows the number of proteins shared by at least two comparison groups (dots of one sector). **(B)** The phylogenetic plot showing the distribution of biological processes in which proteins shared by the comparison groups are involved. Radial ribs correspond to molecular functions; ribs groups denote the biological processes according to their color. Each radial rib corresponds to a specific protein and is denoted with a respective protein-coding gene.

Proteins making the greatest contribution to segmentation of comparison groups can either be classified into the four key biological processes, including lipid transport and metabolism, complement system activation, iron and heme transport, and implementation of adaptive immunity or are acute phase proteins (Figure 3).

3.3 Phosphorylated proteoforms

Post-translational modifications (PTMs) often affect protein function (Nikolsky et al., 2023). In this study, we analyzed the possible phosphorylated proteoforms, one of the most common native protein modifications. Table 6 lists the results of searching for phosphorylated proteoforms, including those carrying phosphorylated serine (SEP), phosphorylated threonine (TPO) and phosphorylated tyrosine (PTR).

Table 6 shows that the phosphorylated proteoform of apolipoprotein B-100 was observed in eight blood biosamples in the KC and KD groups. Such proteoforms as complement factor B (n = 9), prothrombin (n = 6), and transthyretin (n = 5) are also more common in groups with a kidney pathology compared to the control group. Observation of these phosphorylated proteoforms in the investigated blood samples is interesting in terms of their abundance in the comparison groups. Meanwhile, these results do not provide information enabling precise classification of each group of patients with a pathology (KC and KD): occurrence of PTM-containing proteoforms is approximately identical in both groups,
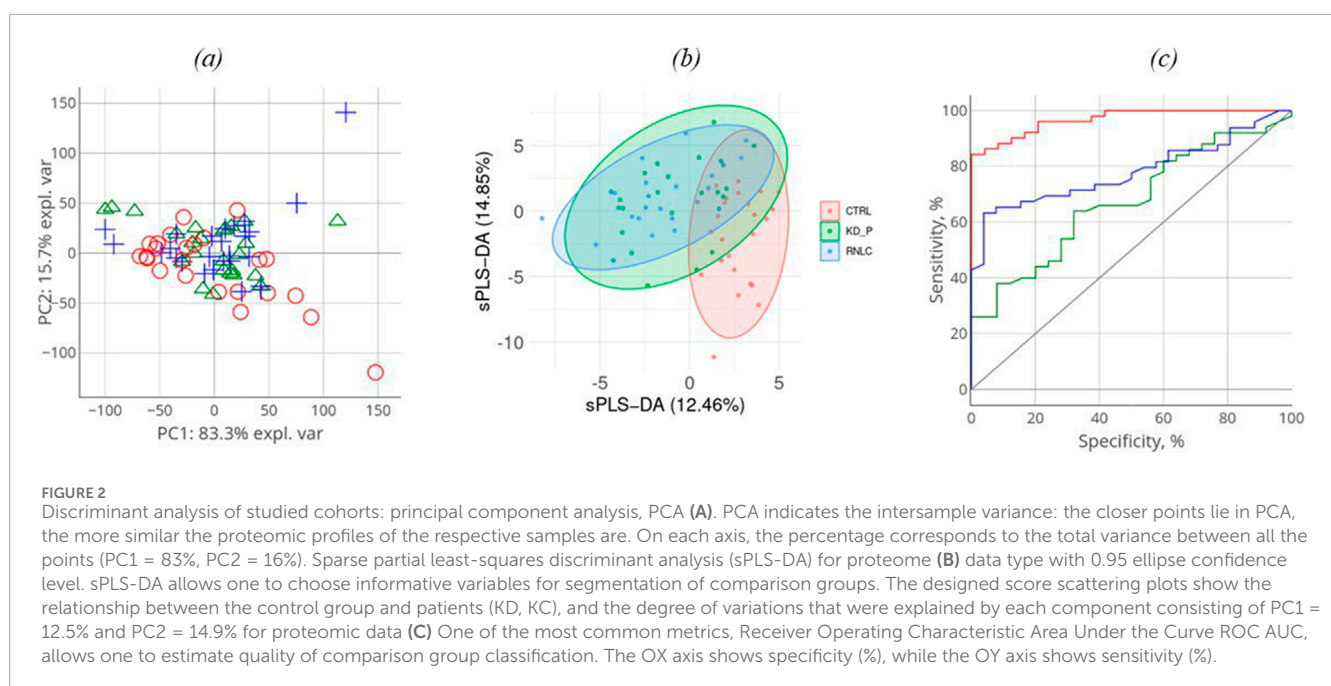
being indicative of the synergistic pathogenesis of the selected groups of urologic diseases (kidney calculus, kidney cyst, and kidney cancer). The results also suggest that this study needs to be continued using a significantly larger number of study subjects (patients having a kidney pathology (KC, KD) and control group (CNTR).

Analysis of the location of a modifying moiety with respect to the interface of binding to native partner proteins (the Interface column) helps assess the potential effect of a PTM on protein structure and functions. Table 7 lists the data on the topology and geometrical parameters of the identified proteoforms. Experimentally determined 3D structures in Protein data bank, including those forming complexes with partner proteins, were identified for four proteins listed in Table 7. For these proteins, it was found that the region carrying modified amino acid residues is located on the protein globule surface and is accessible for interacting with a partner protein. In three cases, the regions carrying modified amino acid residues are located directly at the interface of binding to the partner protein or near the binding site (see Table 7, $K_{SASA} \leq 1$). The K_{SASA} parameter characterizes changes in the solvent-accessible surface area for a peptide in the protein chain and the protein–protein complex. This parameter indirectly indicates the location of peptide (in our case, carrying a modifying moiety) with respect to the interface of binding to the partner protein.

The type of structural motif of the protein comprising the peptide carrying a modifying moiety was identified in each case. Thus, for CFB complexes, the partner of complement factor C4a (PDB ID 2XWJ) modified peptide is located in the dense β-hairpin

TABLE 5 Most significantly altered proteins measured in the study cohorts (estimated as fold changes; |FC| > 1.5, Benjamini−Hochberg adjusted p-value cut-off *p* < 0.05 for one or both comparison groups).

UniProt ID	Gene	Protein	Pathway description	KD		KC	
				Fold changes	Adj. p-value	Fold changes	Adj. p-value
P00751	CFB	Complement factor B	Complement activation, alternative pathway	1.4	0.13	1.7	0.004
P01011	SERPINA3	Alpha-1-antichymotrypsin	Acute-phase response	1.5	0.045	1.4	0.05
P02790	HPX	Hemopexin	Positive regulation of immunoglobulin production	1.5	5.6×10^{-5}	1.4	0.0003
P04196	HRG	Histidine-rich glycoprotein	Positive regulation of immune response to tumor cell	1.4	0.09	1.7	0.02
P05155	SERPING1	Plasma protease C1 inhibitor	Complement activation, classical pathway	1.5	0.003	–	–
P68871	HBB	Hemoglobin subunit beta	Oxygen transport	2.1	0.08	4.1	0.0008
P19652	ORM2	Alpha-1-acid glycoprotein 2	Acute-phase response	1.4	0.02	1.4	0.02
P00450	CP	Ceruloplasmin	Iron ion transport	1.4	0.04	1.3	0.04
P01825	IGHV4-59	Ig	Immunoglobulin-mediated immune response	1.6	0.005	1.5	0.01

FIGURE 2
Discriminant analysis of studied cohorts: principal component analysis, PCA **(A)**. PCA indicates the intersample variance: the closer points lie in PCA, the more similar the proteomic profiles of the respective samples are. On each axis, the percentage corresponds to the total variance between all the points (PC1 = 83%, PC2 = 16%). Sparse partial least-squares discriminant analysis (sPLS-DA) for proteome **(B)** data type with 0.95 ellipse confidence level. sPLS-DA allows one to choose informative variables for segmentation of comparison groups. The designed score scattering plots show the relationship between the control group and patients (KD, KC), and the degree of variations that were explained by each component consisting of PC1 = 12.5% and PC2 = 14.9% for proteomic data **(C)** One of the most common metrics, Receiver Operating Characteristic Area Under the Curve ROC AUC, allows one to estimate quality of comparison group classification. The OX axis shows specificity (%), while the OY axis shows sensitivity (%).

FIGURE 3
Names of the genes encoding proteins contributing most to segmentation of comparison groups clustered with respect to shared biological processes. Arrows show DEPs ($p < 0.05$).

of the beta-containing ribbon functional domain (Figure 4A). In proteins of different organisms, this domain type is involved in formation of protein–protein and protein–nucleic acid complexes (e.g., in zinc finger proteins, where the ribbon domain is stabilized by coordination bonds with a zinc cation) (Li et al., 2022). The K_{SASA} parameter of the CFB/C4a complexes is 0.6, indicating that the revealed CFB peptide carrying a modifying moiety is engaged in organization of the binding interface of the complex. Other members involved in activation of the complement cascade C4a/C4b also form complexes with partner proteins (PDB ID 6YSQ, Figure 4B). The identified modified peptides in the complexes are a part of β-hairpins of the sandwich functional domain. The sandwich functional domain in proteins is also an essential structural participant of protein complex formation (Nikolsky et al., 2024). In our study, the identified peptides carrying a modifying moiety also resided directly in the binding interface ($K_{SASA} = 0.5$) of two complement factors, C4a and C4b. Figure 4C illustrates the prothrombin protein in complex with coagulation factors Va and Xa; the region carrying modified amino acid residues is located in an unstructured domain residing on the protein globule surface. However, the modification site in this complex is remote from the protein binding interface ($K_{SASA} = 1$).

No full-atom models are available for three proteins (APOB, TTR, and NRAP) in PDB. The lack of structural data on these proteins in the PDB and AlphaFold databases makes it difficult to map the phosphorylation site with respect to the interface of binding to the partner protein. However, potential partners (presented in Table 7) were identified for the remaining proteins.

Structural analysis of proteins associated with development of diseases (primarily, cancer) is interesting for researchers (e.g., a recent study of the occurrence of α-helix- and β-strand-carrying structural domains in proteins encoded by over- and underexpressed genes) for 21 cancer types. The authors called this

study "pan-cancer structurome" and demonstrated an increased amount of β-sandwich domains and insufficient amount of α-helices in proteins (Medvedev et al., 2023).

4 Discussion

Kidney diseases are currently extremely common. Although there exists a broad variety of kidney pathologies according to the ICD-10 classification, the literature suggests rather similar clinical presentations of disease development. Moreover, some studies attest to the "mimicry" of kidney diseases (Tseng, 2015; Lu et al., 2021; Lai et al., 2019) and malignant transformation of benign neoplasms (Jiang et al., 2015; Yu et al., 2017). These factors impede diagnosis and timely choice of an efficient treatment option. Histological examination is undoubtedly a potent clinical diagnosis tool providing an unambiguous answer to the question about the neoplasm nature. However, histology cannot be viewed from the standpoint of a routine diagnostic approach, since it is an invasive procedure associated with surgical intervention. It is important to develop novel minimally invasive approaches that would allow one to detect transition from a benign kidney neoplasm to a malignant one. In the present study, we examined changes in protein compositions and proteoforms in three pathologies: kidney cyst, kidney calculus, and kidney cancer. For understanding the molecular differences between the selected pathologies, study subjects involved patients with acquired cysts requiring no surgical intervention for the underlying disease (Bosniak I or II cysts); patients with kidney cancer who predominantly had small-sized tumors and belonged to group T1 (according to the TNM classification); patients in this group had no lymph node metastases (N0). Most patients with kidney calculus were found to have

TABLE 6 Proteins carrying a modifying moiety detected in the analyzed blood samples.

UniProt ID	Protein(s)	Pathways	Sequence variants	PTM loci	CNTR	KC	KD
P04114	Apolipoprotein B-100	Post-translational protein phosphorylation	VKYTLNKNSLK YTLNKNSLK	1287-PTR 1288-TPO	1	5	3
P00751	Complement factor B	Alternative complement activation	LEDSVTYHCSR VGSQYRLEDSVTYHCSR	~183–194	1	4	5
P0C0L5 P0C0L4	Complement C4-B Complement C4-A	Activation of C3 and C5	TTNIQGINLLFSSRR GPEVQLVAHSPWLKDSLSRTTNIQGINLLFSSR DSLSRTTNIQGINLLFSSR	123–138	0	0	2
P02766	Transthyretin	Neutrophil degranulation	DFALLSLQVPLK	86-SER	0	2	1
			LLLLCLAGLVFVSEAGPTGTGESK	25-TPO	0	4	1
Q86VF7	Nebulin-related-anchoring protein	Ion binding	KKLHEYTVLPEDMK KLHEYTVLPEDMKTQWAK	659-PTR 660-TPO	3	0	0
P00734	Prothrombin	Regulation of the complement cascade	GHVNITR GHVNITRSGIECQLWRSR	123-TPO	1	3	3

Pathways–according to the Reactome data; Sequence variants–amino acid sequence variants that were detected in biosamples; PTM, Loci–the localization region or an accurate coordinate of PTM.

medium- and large-sized stones in the kidney and underwent nephrolithotomy.

We can see that the analyzed pathologies are similar at the protein level. A small group of proteins (n = 9) was revealed, which can be classified as differentially expressed proteins (DEPs) compared to the control group. Because of the specific feature of the selected pathologies, these proteins are involved in activation and implementation of the antibody-dependent response of the immune system (GO:0002250) and simultaneous activation of the complement system via the classical pathway (GO:0006958). Proteins (n = 38, |w| >0.1) making the greatest contribution to segmentation of comparison groups, along with the aforementioned biological processes, are involved in the complement (GO:0006956) and coagulation system (GO: 0050817), lipid transport and metabolism (GO:0006629, GO:0006869), or are acute phase proteins (GO:0006953). Although a relatively modest accuracy (70 or 80%) has been achieved in classifying the comparison groups, close attention to the identified protein factors in combination with clinical observations will possibly improve this result. We have generalized the findings and supplemented them with the available data to reconstruct the potential molecular mechanisms for the involvement of proteins identified in this study.

4.1 The complement system

The complement system is the key part of the immunity. Disbalancing of activation regulation of this system may cause inflammation and further development of different diseases (Lin et al., 2018). Patients with various tumor pathologies have increased expression of some complement factors in the classical complement pathway, which contribute to immune surveillance through cytotoxicity and lysis of tumor cells (Afshar-Kharghan, 2017). However, overexpression of the membrane and soluble forms of inhibitors of complement components was observed in the case of solid tumors, protecting the tumor against complement-mediated lysis (Reese et al., 2020). Interestingly, our study revealed increased levels of proteins of the C3/C5 axis, namely, CFB (FC = 1.7, p = 0.004), and C3 (FC = 1.3, uncertain value), C4B (FC = 1.5, uncertain value), Clu (FC = 1.4, p = 0.065), which is consistent with the literature data on prognostic significance of these factors in human kidney cancer (Xi et al., 2016; Netti et al., 2021; Reese et al., 2020). Proteins CFB, C3, C4A, and C4B are associated with the development of kidney diseases (see Supplementary Table S5). Complement activation may induce or promote glomerular injury in multiple kidney diseases (Vivarelli et al., 2024) (Figure 5). However, conspicuous is the fact that the role of the axis in oncogenesis is rather ambiguous, since a number of studies have demonstrated that tumor grows under C3/C5 activation conditions through recruitment and activation of myeloid suppressor cells in tumors (Reis et al., 2018; Pio et al., 2013; Macor et al., 2018; Berraondo et al., 2016). Acute-phase protein alpha-2-macroglobulin (A2M) is another circulating component potentially associated with the C3/C5 axis of complement activation (the classical pathway). It is a multi-functional high-molecular-weight homotetrameric glycoprotein interacting with proteinases, which induces conformational changes in the monomer molecules and modulates their function (Arimura and Funabiki, 2021;

TABLE 7 Structural characterization of the phosphorylation sites in proteins with annotated 3D structures according to the PDB and AlphaFold databases.

Uniprot ID	Peptide seq	Name	Gene	Domain	Motif	Partners	PDB/PDB$_{cmp}$	Location	K_{SASA}	HB	HP	Interface
P00751	LEDSVTYHCSR	Complement factor B	CFB	Ribbon	β-hairpin	Q91132: Cobra venom factor P00746: Complement factor D P01024: Complement C3 P27918: Properdin	10/15	Protein globule surface	0.6 ± 0.05	11 ± 2	8 ± 1	In
P0C0L5	TTNIQGINLLFSSR	Complement C4-B	C4B	Sandwich		P0C0L4: Complement C4-A	2/2	Protein globule surface	0.5 ± 0.01	14 ± 1	29 ± 0	In
	DFALLSLQVPLK				β-hairpin		2/2	Protein globule surface	1.0 ± 0.06	2 ± 0	42 ± 1	Near
P0C0L4	TTNIQGINLLFSSR	Complement C4-A	C4A	Sandwich		O00187: Mannan-binding lectin serine protease 2	2/5	Protein globule surface	0.8 ± 0.2	17 ± 1	30 ± 1	In
	DFALLSLQVPLK						2/5	Protein globule surface	1 ± 0	2 ± 0	44 ± 1	Out
P00734	GHVNITR	Prothrombin	F2	Beta Barrel	Irregular domain	P00742: Coagulation factor X P12259: Coagulation factor V	1/8	Protein globule surface	1 ± 0	7 ± 2	11 ± 2	Out
P04114	PTR-TLNKNSLK Y-TPO-LNKNSLK	Apolipoprotein B-100	APOB	n/d	n/d	Q8NBP7: proprotein convertase subtilisin/kexin type 9 (Sun et al., 2012) P55157: microsomal triglyceride transfer protein large subunit (Walsh et al., 2015) Q9Y679: Lipid droplet-regulating VLDL assembly factor AUP1 (Zhang et al., 2017a)	–	–	–	–	–	–

(Continued on the following page)

TABLE 7 (*Continued*) Structural characterization of the phosphorylation sites in proteins with annotated 3D structures according to the PDB and AlphaFold databases.

Uniprot ID	Peptide seq	Name	Gene	Domain	Motif	Partners	PDB/PDB$_{cmp}$	Location	K$_{SASA}$	HB	HP	Interface
P02766	LLLLCLAGLVFVSEAGP-TPO-GTGESK	Transthyretin	TTR	n/d	n/d	Q15109: Advanced glycosylation end product-specific receptor P05067: Amyloid-beta precursor protein (according to the IntAct database)	–	–	–	–	–	–
Q86VF7	KLHEYTVLPEDMK	Nebulin-related-anchoring protein	NRAP	n/d	n/d	P35609: Alpha-actinin-2 P50461: Cysteine and glycine-rich protein 3 (according to the IntAct database)	–	–	–	–	–	–

Functional domain identifier according to CATH v.4.3 (https://www.cathdb.info/); Motif—a structural motif where the PTM-carrying peptide is located; CATH v.4.3 (https://www.cathdb.info/); Motif—a structural motif where the PTM-carrying peptide is located; PDB—the number of protein structures in PDB; PDB$_{cmp}$—the number of structures in PDB with this peptide containing protein–protein complexes; localization–mapping of the PTM-carrying peptide to the 3D structure of the protein; the coefficient of participation in binding site K$_{SASA}$ is the ratio between SASA of the peptide in the complex and SASA of the peptide in the protein chain. It indirectly characterizes the location of the PTM-carrying peptide with respect to the interface of binding to the partner protein. K$_{SASA}$ < 1 is indicative of participation in the interface with the partner protein; K$_{SASA}$ ≥1 means that the peptide lies outside the binding site; HB is the estimated number of hydrogen bonds between the peptide; Interface is the estimated location of the PTM-carrying peptide with respect to the interface of binding with the partner protein. IntAct database, release 246 (https://www.ebi.ac.uk/intact/home).

Lagrange et al., 2022). The inhibitory mechanism of A2M involves formation of a tetrameric structure around active proteases and physically hampers the interaction between proteases and substrates (the so-called snap-trap mechanism) (Vandooren and Itoh, 2021a). There are parallels between functioning of C3 and C4 factors and A2M. The pivotal element of the system is the cleavage of C3 and C4 factors followed by exposure of internal thioester binding neighboring glycoproteins (Vandooren and Itoh, 2021a). Similar to C3 and C4, A2M undergoes proteolysis and conformational changes to expose internal thioester that binds and entraps active protease (Vandooren and Itoh, 2021b). Along with C3 and C4, A2M is classified as a member of the thioester-containing protein (TEP) family (Vandooren and Itoh, 2021a). All these factors are eventually involved in formation of the membrane attack complex (MAC), which leads to cell lysis and forces cells release inflammatory cytokines. MAC formation is regulated (namely, inhibited) by clusterin protein, which is essential for protecting own cells against being attacked by the MAC during complement activation (Lin et al., 2018).

Protein serine proteinase complement factor B (CFB) is involved in complement activation (Riihilä et al., 2019). CFB binds to C3b and forms the C3bB complex, participates in formation of C3 convertase and further C5 convertase, acting as an activator of the complement system via the alternative pathway (Figure 5). Dysregulation of these processes may lead to hypercoagulation and thrombosis development. Hyperactivation of the alternative complement pathway with involvement of CFB results in the development of C3 glomerulopathy, which leads to accumulation of the C3 component and glomerular injury. Vitronectin (VTN, FC = 1.3, uncertain value), whose expression is upregulated during complement activation (Ruiz-Molina et al., 2023) is a defense protein and an inhibitor of complement activation via the alternative pathway (Figure 5).

4.2 The coagulation system

The proteolytic cascades (the immune system, the complement and the coagulation system) are finely mutually balanced by a network of regulatory factors. The complement–coagulation crosstalk can influence activation, amplification and regulatory functions in both systems (Heurich and McCluskey, 2023). In our study, we noted that proteins of the coagulation system (fibrinogen chain A, B and G (FGA, FGB, FGG, respectively)), as well as phosphorylated prothrombin (F2), contribute to segmentation of the comparison groups. Figure 5 shows the potential mechanism of the crosstalk between the coagulation system and complement factors, the so-called "coagulo-complementome". Prothrombin and thrombin-activatable fibrinolysis inhibitor (TAFI) mediate this interaction (Danckwardt et al., 2013). Blood clotting factors play an important role in cancer biology (Bauer et al., 2022). Coagulation abnormalities are common among cancer patients who have an increased procoagulant activity due to the release of tumor-derived procoagulants into the bloodstream (Danckwardt et al., 2013). Elevated plasma levels of fibrinogen in patients with renal cell carcinoma were reported in the literature (Selby et al., 2018; Chen et al., 2024; Tupikowski et al., 2023; Wang et al., 2020).
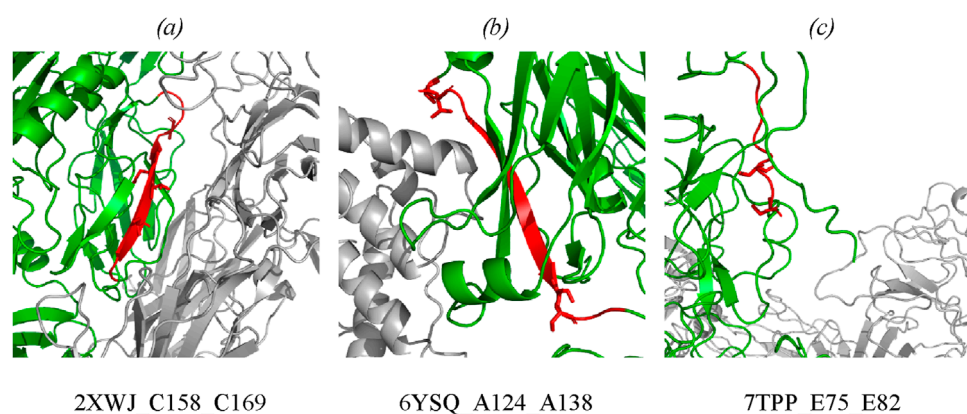
FIGURE 4
Mapping of the identified phosphorylated peptides in protein−protein complexes: **(A)** CFB in complex with complement C4a (PDB: 2XWJ); **(B)** complement C4b in complex with complement C4a (PDB: 6YSQ); **(C)** prothrombin in complex with activated factor Xa and coagulation factor Va (PDB: 7TPP). Modified proteins are shown in green; partners are shown in gray; detected peptides are shown in red; side chains of phosphorylated residues are shown as stick representation. Full data are available in the Supplementary Tables S3, S4.

Plasma protease C1 inhibitor (SerpinG1) belongs to the family of serine protease inhibitors and is an important regulator of the complement, coagulation, and fibrinolytic systems. The blood levels of the protease/SerpinG1 complexes (C1/SerpinG1, Thrombin/SerpinG1) are proportional to the level of activation of these enzyme cascades in blood plasma (Kajdácsi et al., 2020) (Figure 5). In our study, we observed that the SerpinG1 level in renal patients was moderately increased (FC = 1.5, p = 0.003). The "coagulo-complementome" factors show great promise as therapeutic targets and diagnostic factors (Danckwardt et al., 2013).

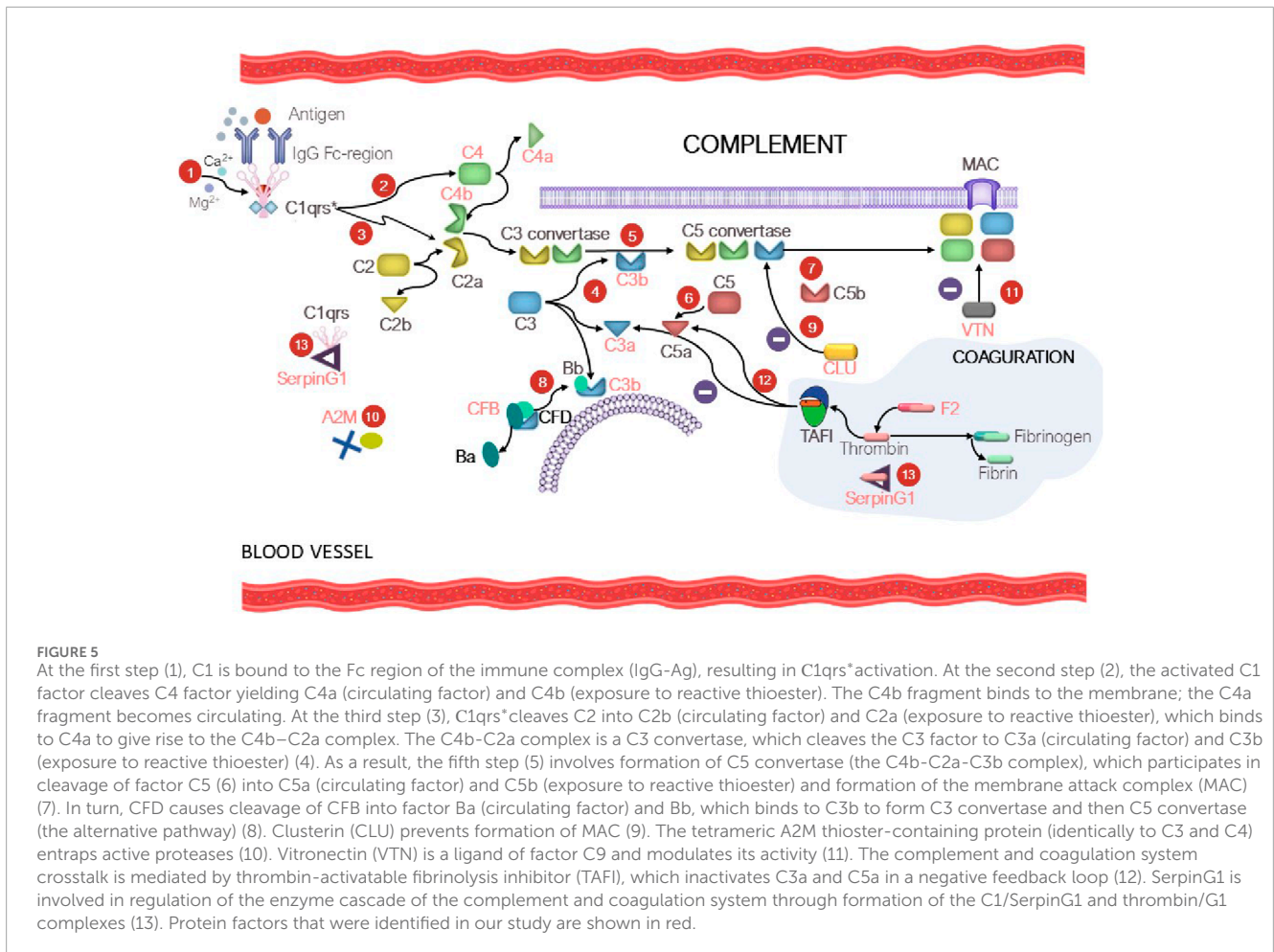### 4.2.1 Lipid transport and metabolism

Lipid metabolism reprogramming is an obvious sign of cancer. Lipids play a crucial role at the cellular (membrane biosynthesis and energy metabolism) and organ levels (intercellular signaling). Modulation of lipid metabolism allows tumor cells to survive in a nutrient-deprived environment (Heravi et al., 2022). Lipid reprogramming in kidney cancer is related to changes in cholesterol (Wu et al., 2019; Saito et al., 2016; Abduljabbar et al., 2024) and fatty acid (Lv et al., 2019; Wu et al., 2020) metabolism as well as lipolysis reduction (Zhang X. et al., 2017). In our study, we observed significant differences in patients' weight and BMI for the KD and KC groups vs. the CNTR group. The mean weight of females in the KD group was 87 ± 12.6 kg; in the KC group, 98 ± 12.3 kg; and in the CNTR group, 65.8 ± 6 kg. In males, a similar weight gain was observed in the KD group (86.5 ± 12.7 kg) and KC group (95 ± 10 kg) vs. the CNTR group (68.5 ± 7 kg) (Table 2). According to their BMI, male and female subjects in the KD and KC groups were overweight or had class 1 and class 2 obesity, respectively. Subjects in CNTR either had normal weight or were overweight. Obesity is a risk factor for kidney cancer; elevated body mass index is associated with poor prognosis (Selby et al., 2018). Along with the risk of developing various cancer types, including kidney cancer, overweight is also associated with developing such comorbidities as nonalcoholic fatty liver disease, hypertension, and type 2 diabetes mellitus. Control over hypertension and obesity, as

well as quitting smoking, are important measures for primary kidney cancer prevention (Gray and Harris, 2019). At the molecular level, we observed significant elevation of blood levels of triglycerides (FC = 3, p = 0.00003) and glucose (FC = 1.4, p = 0.002), as well as increased levels of histidine-rich glycoprotein (HRG, FC = 1.7, p = 0.02) and serum paraoxonase 1 (PON1, FC = 1.5, uncertain value). Insulin resistance, the key component of the metabolic syndrome, as well as elevation of the triglyceride level are associated with kidney cancer. The assessed triglyceride-glucose index is a prognostic factor of survival in patients with postoperative renal cell carcinoma (Qin et al., 2024).

HRG is a plasma protein playing a crucial role in regulating the immune response, angiogenesis, and hemostasis. It is involved in various biological processes due to its ability to interact with heparin, fibrinogen, platelets, immune cells, and growth factors. Disruption of HRG function is associated with various diseases, including breast cancer and hepatocellular carcinoma. HRG dysfunction may promote tumor tissue growth by disrupting the balance between pro- and anti-angiogenic factors. PON1 enzyme is involved in antitumor response; it inhibits migration, invasion and proliferation of kidney cancer cells and suppresses tumor growth (Li and Yu, 2019). These proteins have a wide range of functions, are involved in tumor progression and antitumor response; in the literature, they are regarded as candidate targets for drugs or prognostic predictors (Johnson et al., 2014; Oiwa et al., 2022; Jiang et al., 2021; Schneider et al., 2016).

4.2.2 Acute phase

There is a well-known association between acute phase proteins (APPs) and oncopathology: a positive correlation between the elevated APP level and an unfavorable clinical outcome has been revealed (Janciauskiene et al., 2021a). In this study, we observed elevated levels of alpha-1-antichymotrypsin (SerpinA3, FC = 1.4, p = 0.05), A2M (FC = 1.3, p = 0.02), alpha-1-acid glycoprotein 2 (ORM2, FC = 1.4, p = 0.02), hemopexin (HP, FC = 4, uncertain value), and ceruloplasmin (CP, FC = 1.3, p = 0.04). These proteins are probably

FIGURE 5
At the first step (1), C1 is bound to the Fc region of the immune complex (IgG-Ag), resulting in C1qrs*activation. At the second step (2), the activated C1 factor cleaves C4 factor yielding C4a (circulating factor) and C4b (exposure to reactive thioester). The C4b fragment binds to the membrane; the C4a fragment becomes circulating. At the third step (3), C1qrs*cleaves C2 into C2b (circulating factor) and C2a (exposure to reactive thioester), which binds to C4a to give rise to the C4b−C2a complex. The C4b-C2a complex is a C3 convertase, which cleaves the C3 factor to C3a (circulating factor) and C3b (exposure to reactive thioester) (4). As a result, the fifth step (5) involves formation of C5 convertase (the C4b-C2a-C3b complex), which participates in cleavage of factor C5 (6) into C5a (circulating factor) and C5b (exposure to reactive thioester) and formation of the membrane attack complex (MAC) (7). In turn, CFD causes cleavage of CFB into factor Ba (circulating factor) and Bb, which binds to C3b to form C3 convertase and then C5 convertase (the alternative pathway) (8). Clusterin (CLU) prevents formation of MAC (9). The tetrameric A2M thioster-containing protein (identically to C3 and C4) entraps active proteases (10). Vitronectin (VTN) is a ligand of factor C9 and modulates its activity (11). The complement and coagulation system crosstalk is mediated by thrombin–activatable fibrinolysis inhibitor (TAFI), which inactivates C3a and C5a in a negative feedback loop (12). SerpinG1 is involved in regulation of the enzyme cascade of the complement and coagulation system through formation of the C1/SerpinG1 and thrombin/G1 complexes (13). Protein factors that were identified in our study are shown in red.

associated with the development of different oncopathologies and are viewed in the literature as candidate biomarkers for cancer prognosis and diagnosis of complications of cancer treatment (Janciauskiene et al., 2021a; Lu et al., 2016; Han et al., 2017; Ohbatake et al., 2016; Janciauskiene et al., 2021b). SerpinA3 is a serine protease inhibitor involved in regulation of inflammation and proteolytic activity. In the context of oncopathology, this protein may modulate the tumor microenvironment by inhibiting proteases involved in extracellular matrix degradation. SerpinA3, as well as A2M, alpha-1-acid glycoprotein 2, are considered candidate biomarkers of various cancers, including kidney cancer (Jin et al., 2022; Aibara et al., 2021). Hemopexin is also a circulating protein that plays an important role in protecting the body against heme toxicity during hemolysis. In patients with acute kidney injury, HP compensates for oxidative stress, inflammation, and apoptosis of renal tubular cells as a result of heme accumulation. However, HP deficiency may increase the risk of acute kidney failure progression and development of secondary damage such as diabetic nephropathy. ORM2 is a plasma protein playing a crucial role in regulation of inflammation and immune response. Copper-binding protein CP (ceruloplasmin) is involved in iron and copper metabolism as well as the antioxidant defense of the body. The protein is involved in regulation of redox

processes, including oxidation of Fe^{2+} to Fe^{3+}, which is required for iron binding to transferrin. Disturbances in ceruloplasmin expression or function are associated with a number of diseases, including aceruloplasminemia, cirrhosis, and Parkinson's disease. IGHV4-59 (FC = 1.6, p = 0.005) is the gene encoding one of immunoglobulin heavy chain variable regions and being involved in immunoglobulin-mediated immune response. The IGHV4-59 gene is engaged in the development of such pathologies as celiac disease and type 2 diabetes mellitus.

4.2.3 Modified proteoforms

Identification of disease-specific proteoforms is important for understanding the nature of oncopathology. There currently is lack of research into identification of modified proteoforms in patients with kidney cancer. In this study, we focused on phosphorylated forms of proteins involved in regulation of the complement system and protein phosphorylation: ApoB, CFB, C4A/C4B, TTR, and NRAP. Structural analysis was conducted for proteins with the annotated 3D structure in the open-source PDB (https://rcsb.org) and AlphaFold (https://alphafold.ebi.ac.uk/) databases, which showed that the modifying moiety resides in β structure-containing structural domains of the ribbon, sandwich, and β-barrel types (according to the CATH database, https://www.cathdb.info/). In

nature, these structural domains are involved in organization of protein- or ligand-binding functional domains. Interestingly, the phosphorylation site in the detected proteins is solvent-oriented. An analysis of structural complexes of the identified proteoforms with native partners demonstrated that the modification site can be mapped directly at the interface of binding to the partner or immediately adjacent to it. Phosphorylation often leads to modulation of protein function both in normal and pathological conditions. The location of the modification site at the protein binding interface is indirectly indicative of changes in complex stability (Nikolsky et al., 2023). In the literature, these modification variants are found in various oncopathologies. Thus, according to the PhosphoSitePlus data (Hornbeck et al., 2019), the identified modification variants ApoB 1287-PTR/1288-TPO and TTR 25-TPO were found in biosamples collected from patients with T-cell leukemia; CFB phosphorylation variants were annotated in patients with gastric carcinoma; C4A/C4B and F2 proteins phosphorylated at other sites were identified in breast, ovarian, stomach, head/neck, and colorectal cancers.

Hence, proteins presented in this study can potentially be associated with the development of kidney diseases; it is promising to conduct further analysis of their medical significance with a larger sample size and number of comparison groups. The results of analyzing the association between the identified proteins and development of various diseases and disease groups in accordance with the ICD-10 classification using the Diseases database (Disease–gene associations mined from literature) (Pletscher-Frankild et al., 2015) are reported in Supplementary Table S5. This analysis revealed that proteins described in our study are most commonly mentioned in the literature in the context of developing cancer, diabetes mellitus, kidney diseases, and hypertension.

5 Conclusion

This study addresses the features of the protein profile of plasma samples collected from patients with kidney diseases. During the study, we conducted proteomic analysis of blood samples in three comparison groups of study subjects: those with verified diagnosis of kidney calculus, kidney cyst or kidney cancer as well as conditionally healthy volunteers. Blood chemistry parameters in all three groups of study subjects (KC, KD and CNTR) were analyzed at the first stage of the study. Blood chemistry parameters in all the groups of study subjects were normal. Plasma proteins were analyzed at the next stage. DEPs whose blood level was found to be elevated with respect to that in the control group were identified. Hemoglobin subunit beta was found to increase most significantly: its level rose more than twofold ($p = 0.08$) in the KD group and more than fourfold ($p = 0.0008$) in the KC group.

We have identified proteins contributing most significantly to pathology development, which allowed us to classify patients with analyzed pathologies into groups. CFB, SERPINA3, HPX, HRG, SERPING1, HBB, ORM2, and CP proteins associated with the development of kidney pathologies have been proposed. Important biological processes have been described, and probable signaling pathways of pathology development involving the identified proteins have been elucidated. The paper summarizes important

biological processes involving the identified proteins: classical antibody-mediated complement activation (R-HSA-173623, n = 46); FCGR activation (R-HSA-2029481, n = 45); as well as binding and uptake of ligands by scavenger receptors (R-HSA-2173782, n = 54).

The third stage of the study involved searching for and analyzing phosphorylated proteoforms. Phosphorylated proteoforms (CFB, C4A/C4B, F2, APOB, TTR, and NRAP) have been detected in the studied blood samples. Phosphorylated proteoforms specific to groups of patients with kidney diseases were analyzed. PTM location in protein was determined: its coordinate, the secondary structure/structural motif, the functional domain, and the potential role in formation of complexes with native partners. The effect of phosphorylation on protein geometry (changes in solvent-accessible surface area; the number of hydrophobic interactions and hydrogen bonds between the PTM-carrying peptide and the remaining protein portion) was analyzed. It has been demonstrated that peptides carrying modified amino acid residues can reside at the interface of binding to the partner protein or near the binding site. An analysis of modified proteins shows synergism in the pathogenesis of selected disease groups.

It has been demonstrated that patients with kidney pathologies can be classified into groups with an accuracy of (70–80)%. Larger size of comparison groups will enable more clear segmentation of the analyzed pathologies and, therefore, allow one to find a faster solution to the problem of early diagnosis of a particular kidney disease in practical medicine.

Data availability statement

The data presented in the study are deposited in the ProteomeXchange Consortium via the PRIDE repository, accession number PXD051799.

Ethics statement

The studies involving humans were approved by the Local Ethics Committee of the Sechenov University (protocol No. 10-19 dated July 17, 2019). The studies were conducted in accordance with the local legislation and institutional requirements, and all handlings and use of material were provided according to the WMA Declaration of Helsinki on Ethical Principles for Medical Research Involving Human Subjects (revision Fortaleza, 2013). The participants provided their written informed consent to participate in this study. Written informed consent was obtained from the individual(s) for the publication of any potentially identifiable images or data included in this article.

Author contributions

KN: Investigation, Methodology, Writing–original draft. ArK: Conceptualization, Investigation, Methodology, Writing–review and editing. VN: Investigation, Writing–original draft. NP: Formal Analysis, Investigation, Writing–original draft. DE: Methodology,

Writing–original draft. TB: Formal Analysis, Writing–original draft. LK: Formal Analysis, Writing–review and editing. KM: Methodology, Writing–original draft. VR: Formal Analysis, Writing–original draft. DP: Formal Analysis, Writing–original draft. AI: Investigation, Writing–original draft. AnK: Conceptualization, Project administration, Writing–original draft.

Funding

Acknowledgments

Conflict of interest

The authors declare that the research was conducted in the absence of any commercial or financial relationships that could be construed as a potential conflict of interest.

Publisher's note

All claims expressed in this article are solely those of the authors and do not necessarily represent those of their affiliated organizations, or those of the publisher, the editors and the reviewers. Any product that may be evaluated in this article, or claim that may be made by its manufacturer, is not guaranteed or endorsed by the publisher.

Supplementary material

The Supplementary Material for this article can be found online at: https://www.frontiersin.org/articles/10.3389/fmolb.2024.1494779/full#supplementary-material

References

Abbiss, H., Maker, G. L., and Trengove, R. D. (2019). Metabolomics approaches for the diagnosis and understanding of kidney diseases. *Metabolites* 9, 34. doi:10.3390/metabo9020034

Abduljabbar, M. K., Merza, M., Aziz, A., Menon, S. V., Kaur, M., Aminov, Z., et al. (2024). Lipid metabolism reprogramming in renal cell carcinomas. *Med. Oncol. N. Lond. Engl.* 41, 243. doi:10.1007/s12032-024-02484-5

Afshar-Kharghan, V. (2017). The role of the complement system in cancer. *J. Clin. Invest.* 127, 780–789. doi:10.1172/JCI90962

Aibara, N., Miyata, Y., Araki, K., Sagara, Y., Mitsunari, K., Matsuo, T., et al. (2021). Detection of novel urine markers using immune complexome analysis in bladder cancer patients: a preliminary study. *Vivo Athens Greece* 35, 2073–2080. doi:10.21873/invivo.12476

Alelign, T., and Petros, B. (2018). Kidney stone disease: an update on current concepts. *Adv. Urol.* 2018, 3068365. doi:10.1155/2018/3068365

Al-Hamed, M. H., Alsahan, N., Rice, S. J., Edwards, N., Nooreddeen, E., Alotaibi, M., et al. (2019). Bialleleic PKD1 mutations underlie early-onset autosomal dominant polycystic kidney disease in Saudi Arabian families. *Pediatr. Nephrol. Berl. Ger.* 34, 1615–1623. doi:10.1007/s00467-019-04267-x

Allegrini, S., Garcia-Gil, M., Pesi, R., Camici, M., and Tozzi, M. G. (2022). The good, the bad and the new about uric acid in cancer. *Cancers* 14, 4959. doi:10.3390/cancers14194959

Arimura, Y., and Funabiki, H. (2021). Structural mechanics of the alpha-2-macroglobulin transformation. *J. Mol. Biol.* 434, 167413. doi:10.1016/j.jmb.2021.167413

Bai, C., Wang, H., Dong, D., Li, T., Yu, Z., Guo, J., et al. (2021). Urea as a by-product of ammonia metabolism can Be a potential serum biomarker of hepatocellular carcinoma. *Front. Cell Dev. Biol.* 9, 650748. doi:10.3389/fcell.2021.650748

Bauer, A. T., Gorzelanny, C., Gebhardt, C., Pantel, K., and Schneider, S. W. (2022). Interplay between coagulation and inflammation in cancer: limitations and therapeutic opportunities. *Cancer Treat. Rev.* 102, 102322. doi:10.1016/j.ctrv.2021.102322

Benjamini, Y., and Hochberg, Y. (1995). Controlling the false discovery rate: a practical and powerful approach to multiple testing. *J. R. Stat. Soc. Ser. B Methodol.* 57, 289–300. doi:10.1111/j.2517-6161.1995.tb02031.x

Bergmann, C., Guay-Woodford, L. M., Harris, P. C., Horie, S., Peters, D. J. M., and Torres, V. E. (2018). Polycystic kidney disease. *Nat. Rev. Dis. Primer* 4, 50–24. doi:10.1038/s41572-018-0047-y

Berraondo, P., Minute, L., Ajona, D., Corrales, L., Melero, I., and Pio, R. (2016). Innate immune mediators in cancer: between defense and resistance. *Immunol. Rev.* 274, 290–306. doi:10.1111/imr.12464

Boo, H. J., Lee, J. E., Chung, S. M., Jang, H. R., Huh, W., Kim, D. J., et al. (2022). The presence of simple renal cysts is associated with an increased risk of albuminuria in young adults. *Korean J. Intern. Med.* 37, 425–433. doi:10.3904/kjim.2020.576

Bratslavsky, G., Mendhiratta, N., Daneshvar, M., Brugarolas, J., Ball, M. W., Metwalli, A., et al. (2021). Genetic risk assessment for hereditary renal cell carcinoma: clinical consensus statement. *Cancer* 127, 3957–3966. doi:10.1002/cncr.33679

Brewin, A., Sriprasad, S., and Somani, B. K. (2021). Role of urinary biomarkers for diagnosis and prognosis of kidney stone disease. *Curr. Opin. Urol.* 31, 71–79. doi:10.1097/MOU.0000000000000856

Brierley, J. D., Gospodarowicz, M. K., and Wittekind, C. (2017). *TNM classification of malignant tumours, 8th edition*. Wiley. Available at: https://www.wiley.com/en-us/TNM+Classification+of+Malignant+Tumours%2C+8th+Edition-p-9781119263579.

Chen, W., Zhao, X., Lu, Y., Wang, H., Wang, X., Wang, Y., et al. (2024). Clinical significance, molecular characterization, and immune microenvironment analysis of coagulation-related genes in clear cell renal cell carcinoma. *Cancer Innov.* 3, e105. doi:10.1002/cai2.105

Chen, Z., Shao, Y., Yao, H., Zhuang, Q., Wang, K., Xing, Z., et al. (2017). Preoperative albumin to globulin ratio predicts survival in clear cell renal cell carcinoma patients. *Oncotarget* 8, 48291–48302. doi:10.18632/oncotarget.15162

Cirillo, L., Innocenti, S., and Becherucci, F. (2024). Global epidemiology of kidney cancer. *Nephrol. Dial. Transpl.* 39, 920–928. doi:10.1093/ndt/gfae036

Claps, G., Faouzi, S., Quidville, V., Chehade, F., Shen, S., Vagner, S., et al. (2022). The multiple roles of LDH in cancer. *Nat. Rev. Clin. Oncol.* 19, 749–762. doi:10.1038/s41571-022-00686-2

Dai, X.-Y., He, Q.-S., Jing, Z., and Yuan, J.-Q. (2020). Serum uric acid levels and risk of kidney cancer incidence and mortality: a prospective cohort study. *Cancer Med.* 9, 5655–5661. doi:10.1002/cam4.3214

Danckwardt, S., Hentze, M. W., and Kulozik, A. E. (2013). Pathologies at the nexus of blood coagulation and inflammation: thrombin in hemostasis, cancer, and beyond. *J. Mol. Med.* 91, 1257–1271. doi:10.1007/s00109-013-1074-5

Devi, A. T., Nagaraj, R., Prasad, A., Lakkappa, D. B., Zameer, F., and Nagalingaswamy, N. P. M. (2023). Nephrolithiasis: insights into biomimics, pathogenesis, and pharmacology. *Clin. Complement. Med. Pharmacol.* 3, 100077. doi:10.1016/j.ccmp.2022.100077

Dillman, J. R., Trout, A. T., Smith, E. A., and Towbin, A. J. (2017). Hereditary renal cystic disorders: imaging of the kidneys and beyond. *Rev. Publ. Radiol. Soc. N. Am. Inc.* 37, 924–946. doi:10.1148/rg.2017160148

Ding, T., Zhao, T., Li, Y., Liu, Z., Ding, J., Ji, B., et al. (2021). Vitexin exerts protective effects against calcium oxalate crystal-induced kidney pyroptosis *in vivo* and *in vitro*. *Phytomedicine Int. J. Phytother. Phytopharm.* 86, 153562. doi:10.1016/j.phymed.2021.153562

EAU (2024a). *EAU-Guidelines-on-Renal-Cell-Carcinoma-2024.pdf*.

EAU (2024b). *EAU-Guidelines-on-Urolithiasis-2024.pdf*.

Eliseev, J. J. (2023). *Analizy. Polnyj medicinskij spravochnik. Kljuchevye laboratornye issledovanija v odnoj knige (Russ)*. Moscow: Eksmo. ISBN: 978-5-04-170669-2EAN:9785041706692.

Ferlay, J., Colombet, M., Soerjomataram, I., Dyba, T., Randi, G., Bettio, M., et al. (2018). Cancer incidence and mortality patterns in Europe: estimates for 40 countries and 25 major cancers in 2018. *Eur. J. Cancer Oxf. Engl. 1990* 103, 356–387. doi:10.1016/j.ejca.2018.07.005

Garfield, K., and Leslie, S. W. (2024). "Simple renal cyst," in *StatPearls* (Treasure Island (FL): StatPearls Publishing).

Gray, R. E., and Harris, G. T. (2019). Renal cell carcinoma: diagnosis and management. *Am. Fam. Physician* 99, 179–184.

Han, I. W., Jang, J. Y., Kwon, W., Park, T., Kim, Y., Lee, K. B., et al. (2017). Ceruloplasmin as a prognostic marker in patients with bile duct cancer. *Oncotarget* 8, 29028–29037. doi:10.18632/oncotarget.15995

Heravi, G., Yazdanpanah, O., Podgorski, I., Matherly, L. H., and Liu, W. (2022). Lipid metabolism reprogramming in renal cell carcinoma. *Cancer Metastasis Rev.* 41, 17–31. doi:10.1007/s10555-021-09996-w

Heurich, M., and McCluskey, G. (2023). Complement and coagulation crosstalk – factor H in the spotlight. *Immunobiology* 228, 152707. doi:10.1016/j.imbio.2023.152707

Hornbeck, P. V., Kornhauser, J. M., Latham, V., Murray, B., Nandhikonda, V., Nord, A., et al. (2019). 15 years of PhosphoSitePlus®: integrating post-translationally modified sites, disease variants and isoforms. *Nucleic Acids Res.* 47, D433–D441. doi:10.1093/nar/gky1159

Howles, S. A., and Thakker, R. V. (2020). Genetics of kidney stone disease. *Nat. Rev. Urol.* 17, 407–421. doi:10.1038/s41585-020-0332-x

Janciauskiene, S., Wrenger, S., Günzel, S., Gründing, A. R., Golpon, H., and Welte, T. (2021a). Potential roles of acute phase proteins in cancer: why do cancer cells produce or take up exogenous acute phase protein alpha1-antitrypsin? *Front. Oncol.* 11, 622076. doi:10.3389/fonc.2021.622076

Janciauskiene, S., Wrenger, S., Günzel, S., Gründing, A. R., Golpon, H., and Welte, T. (2021b). Potential roles of acute phase proteins in cancer: why do cancer cells produce or take up exogenous acute phase protein alpha1-antitrypsin? *Front. Oncol.* 11, 622076. doi:10.3389/fonc.2021.622076

Jiang, C., Zhang, X., Li, X., Li, J., and Huang, H. (2021). High PON1 expression predicts poor prognosis in kidney renal clear cell carcinoma. *Res. Square*. doi:10.21203/rs.3.rs-1112733/v1

Jiang, P., Wang, C., Chen, S., Li, J., Xiang, J., and Xie, L. (2015). Primary renal squamous cell carcinoma mimicking the renal cyst: a case report and review of the recent literature. *BMC Urol.* 15, 69. doi:10.1186/s12894-015-0064-z

Jin, Y., Wang, W., Wang, Q., Zhang, Y., Zahid, K. R., Raza, U., et al. (2022). Alpha-1-antichymotrypsin as a novel biomarker for diagnosis, prognosis, and therapy prediction in human diseases. *Cancer Cell Int.* 22, 156. doi:10.1186/s12935-022-02572-4

Johnson, L. D. S., Goubran, H. A., and Kotb, R. R. (2014). Histidine rich glycoprotein and cancer: a multi-faceted relationship. *Anticancer Res.* 34, 593–603.

Kajdácsi, E., Jandrasics, Z., Veszeli, N., Makó, V., Koncz, A., Gulyás, D., et al. (2020). Patterns of C1-inhibitor/plasma serine protease complexes in healthy humans and in hereditary angioedema patients. *Front. Immunol.* 11, 794. doi:10.3389/fimmu.2020.00794

Katwal, B., Gautam, N., Shrestha, S., Singh, L., Gautam, R. K., Adhikari, R., et al. (2022). Biochemical and hemodynamic characterization of nephrolithiasis patients visiting national transplant centre, bhaktapur, Nepal. *Nepal Med. Coll. J.* 24, 276–282. doi:10.3126/nmcj.v24i4.50577

Kc, M., and Leslie, S. W.(2024). "Uric acid nephrolithiasis," in *StatPearls* (Treasure Island (FL): StatPearls Publishing).

Kim, S.-M., Chung, T.-H., Oh, M.-S., Kwon, S.-G., and Bae, S.-J. (2014). Relationship of simple renal cyst to hypertension. *Korean J. Fam. Med.* 35, 237–242. doi:10.4082/kjfm.2014.35.5.237

Kopylov, A. T., Stepanov, A. A., Butkova, T. V., Malsagova, K. A., Zakharova, N. V., Kostyuk, G. P., et al. (2023). Consolidation of metabolomic, proteomic, and GWAS data in connective model of schizophrenia. *Sci. Rep.* 13, 2139. doi:10.1038/s41598-023-29117-7

Lagrange, J., Lecompte, T., Knopp, T., Lacolley, P., and Regnault, V. (2022). Alpha-2-macroglobulin in hemostasis and thrombosis: an underestimated old double-edged sword. *J. Thromb. Haemost.* 20, 806–815. doi:10.1111/jth.15647

Lai, S., Jiao, B., Wang, X., Xu, X., Zhang, M., Diao, T., et al. (2019). Renal cell carcinoma originating in the free wall of simple renal cyst: two unusual case reports with literature review. *Med. Baltim.* 98, e15249. doi:10.1097/MD.0000000000015249

Li, L., Mao, Y., Zhao, L., Li, L., Wu, J., Zhao, M., et al. (2019). p53 regulation of ammonia metabolism through urea cycle controls polyamine biosynthesis. *Nature* 567, 253–256. doi:10.1038/s41586-019-0996-7

Li, X., Han, M., Zhang, H., Liu, F., Pan, Y., Zhu, J., et al. (2022). Structures and biological functions of zinc finger proteins and their roles in hepatocellular carcinoma. *Biomark. Res.* 10, 2. doi:10.1186/s40364-021-00345-1

Li, X., and Yu, Q. (2019). PON1 hypermethylation is associated with progression of renal cell carcinoma. *J. Cell. Mol. Med.* 23, 6646–6657. doi:10.1111/jcmm.14537

Lin, C.-J., Hu, Z.-G., Yuan, G.-D., Lei, B., and He, S.-Q. (2018). Complements are involved in alcoholic fatty liver disease, hepatitis and fibrosis. *World J. Hepatol.* 10, 662–669. doi:10.4254/wjh.v10.i10.662

Liu, L., Zhu, M., Meng, Q., Wang, Y., Zhao, Y., Xie, D., et al. (2020). Association between kidney function and the risk of cancer: results from the China Health and Retirement longitudinal study (CHARLS). *J. Cancer* 11, 6429–6436. doi:10.7150/jca.47175

Lu, J., Wang, Y., Yan, M., Feng, P., Yuan, L., Cai, Y., et al. (2016). High serum haptoglobin level is associated with tumor progression and predicts poor prognosis in non-small cell lung cancer. *Oncotarget* 7, 41758–41766. doi:10.18632/oncotarget.9676

Lu, Y., Hu, J., and Feng, N. (2021). Evolution of renal cyst to renal carcinoma: a case report and review of literature. *Int. J. Clin. Exp. Pathol.* 14, 463–468.

Luo, L., Kieneker, L. M., van der Vegt, B., Bakker, S. J. L., Gruppen, E. G., Casteleijn, N. F., et al. (2023b). Urinary albumin excretion and cancer risk: the PREVEND cohort study. *Nephrol. Dial. Transpl.* 38, 2723–2732. doi:10.1093/ndt/gfad107

Luo, L., Yang, Y., Kieneker, L. M., Janse, R. J., Bosi, A., Mazhar, F., et al. (2023a). Albuminuria and the risk of cancer: the Stockholm CREAtinine Measurements (SCREAM) project. *Clin. Kidney J.* 16, 2437–2446. doi:10.1093/ckj/sfad145

Lv, Q., Wang, G., Zhang, Y., Han, X., Li, H., Le, W., et al. (2019). FABP5 regulates the proliferation of clear cell renal cell carcinoma cells via the PI3K/AKT signaling pathway. *Int. J. Oncol.* 54, 1221–1232. doi:10.3892/ijo.2019.4721

Macor, P., Capolla, S., and Tedesco, F. (2018). Complement as a biological tool to control tumor growth. *Front. Immunol.* 9, 2203. doi:10.3389/fimmu.2018.02203

Malsagova, K. A., Kopylov, A. T., Pustovoyt, V. I., Balakin, E. I., Yurku, K. A., Stepanov, A. A., et al. (2024). Proteomic and metabolomic analyses of the blood samples of highly trained athletes. *Data* 9, 15. doi:10.3390/data9010015

Mangolini, A., de Stephanis, L., and Aguiari, G. (2016). Role of calcium in polycystic kidney disease: from signaling to pathology. *World J. Nephrol.* 5, 76–83. doi:10.5527/wjn.v5.i1.76

Mann, H. B., and Whitney, D. R. (1947). On a test of whether one of two random variables is stochastically larger than the other. *Ann. Math. Stat.* 18, 50–60. doi:10.1214/aoms/1177730491

Medvedev, K. E., Schaeffer, R. D., Chen, K. S., and Grishin, N. V. (2023). Pan-cancer structurome reveals overrepresentation of beta sandwiches and underrepresentation of alpha helical domains. *Sci. Rep.* 13, 11988. doi:10.1038/s41598-023-39273-5

Meguro, S., Koguchi, T., Hakozaki, Y., Onagi, A., Matsuoka, K., Hoshi, S., et al. (2023). Concurrent reduced expression of contiguous PKD1, TSC2 and NTHL1 leading to kidney diseases and multiple diverse renal cancers. *Cancer Genomics Proteomics* 20, 40–50. doi:10.21873/cgp.20363

Mishra, D., and Banerjee, D. (2019). Lactate dehydrogenases as metabolic links between tumor and stroma in the tumor microenvironment. *Cancers* 11, 750. doi:10.3390/cancers11060750

mixOmics (2024). (s)PLS-DA | mixOmics. Available at: http://mixomics.org/methods/spls-da/.

mixOmics Vignette (2024). *7 P-Integration | mixOmics Vignette*.

Moch, H., Cubilla, A. L., Humphrey, P. A., Reuter, V. E., and Ulbright, T. M. (2016). The 2016 WHO classification of tumours of the urinary system and male genital organs-Part A: renal, penile, and testicular tumours. *Eur. Urol.* 70, 93–105. doi:10.1016/j.eururo.2016.02.029

Moftakhar, L., Jafari, F., Ghoddusi Johari, M., Rezaeianzadeh, R., Hosseini, S. V., and Rezaianzadeh, A. (2022). Prevalence and risk factors of kidney stone disease in population aged 40–70 years old in Kharameh cohort study: a cross-sectional population-based study in southern Iran. *BMC Urol.* 22, 205. doi:10.1186/s12894-022-01161-x

Mok, Y., Ballew, S. H., Sang, Y., Coresh, J., Joshu, C. E., Platz, E. A., et al. (2020). Albuminuria, kidney function, and cancer risk in the community. *Am. J. Epidemiol.* 189, 942–950. doi:10.1093/aje/kwaa043

Nagendra, V., Dhande, R., Mishra, G., Reddy, N. G., and Gowda, H. (2023). Hematuria as a sign of kidney stone disease evaluated using computed tomography: a review. *Cureus* 15, e38064. doi:10.7759/cureus.38064

Netti, G. S., Franzin, R., Stasi, A., Spadaccino, F., Dello Strologo, A., Infante, B., et al. (2021). Role of complement in regulating inflammation processes in renal and prostate cancers. *Cells* 10, 2426. doi:10.3390/cells10092426

Nikolsky, K. S., Kulikova, L. I., Petrovskiy, D. V., Rudnev, V. R., Butkova, T. V., Malsagova, K. A., et al. (2024). Three-helix bundle and SH3-type barrels: autonomously

stable structural motifs in small and large proteins. *J. Biomol. Struct. Dyn.* 42, 9090–9104. doi:10.1080/07391102.2023.2250450

Nikolsky, K. S., Kulikova, L. I., Petrovskiy, D. V., Rudnev, V. R., Malsagova, K. A., and Kaysheva, A. L. (2023). Analysis of structural changes in the protein near the phosphorylation site. *Biomolecules* 13, 1564. doi:10.3390/biom13111564

Ohbatake, Y., Fushida, S., Tsukada, T., Kinoshita, J., Oyama, K., Hayashi, H., et al. (2016). Elevated alpha1-acid glycoprotein in gastric cancer patients inhibits the anticancer effects of paclitaxel, effects restored by co-administration of erythromycin. *Clin. Exp. Med.* 16, 585–592. doi:10.1007/s10238-015-0387-9

Oiwa, M., Kuroda, K., Kawanoue, N., and Morimatsu, H. (2022). Histidine-rich glycoprotein as a novel predictive biomarker of postoperative complications in intensive care unit patients: a prospective observational study. *BMC Anesthesiol.* 22, 232. doi:10.1186/s12871-022-01774-7

Palsson, R., Indridason, O. S., Edvardsson, V. O., and Oddsson, A. (2019). Genetics of common complex kidney stone disease: insights from genome-wide association studies. *Urolithiasis* 47, 11–21. doi:10.1007/s00240-018-1094-2

Pan, S., Yuan, T., Xia, Y., Yu, W., Li, H., Rao, T., et al. (2024). SMYD2 promotes calcium oxalate-induced glycolysis in renal tubular epithelial cells via PTEN methylation. *Biomedicines* 12, 2279. doi:10.3390/biomedicines12102279

Park, H. C., Ryu, H., Kim, Y. C., Ahn, C., Lee, K. B., Kim, Y. H., et al. (2021). Genetic identification of inherited cystic kidney diseases for implementing precision medicine: a study protocol for a 3-year prospective multicenter cohort study. *BMC Nephrol.* 22, 2. doi:10.1186/s12882-020-02207-8

Perez-Riverol, Y., Bai, J., Bandla, C., García-Seisdedos, D., Hewapathirana, S., Kamatchinathan, S., et al. (2021). The PRIDE database resources in 2022: a hub for mass spectrometry-based proteomics evidences. *Nucleic Acids Res.* 50, D543–D552. doi:10.1093/nar/gkab1038

Pio, R., Ajona, D., and Lambris, J. D. (2013). Complement inhibition in cancer therapy. *Semin. Immunol.* 25, 54–64. doi:10.1016/j.smim.2013.04.001

Pletscher-Frankild, S., Pallejà, A., Tsafou, K., Binder, J. X., and Jensen, L. J. (2015). DISEASES: text mining and data integration of disease–gene associations. *Methods* 74, 83–89. doi:10.1016/j.ymeth.2014.11.020

Qin, G., Sun, Z., Jin, Y., Ren, X., Zhang, Z., Wang, S., et al. (2024). The association between the triglyceride–glucose index and prognosis in postoperative renal cell carcinoma patients: a retrospective cohort study. *Front. Endocrinol.* 15, 1301703. doi:10.3389/fendo.2024.1301703

Reese, B., Silwal, A., Daugherity, E., Daugherity, M., Arabi, M., Daly, P., et al. (2020). Complement as prognostic biomarker and potential therapeutic target in renal cell carcinoma. *J. Immunol. Balt. Md 1950* 205, 3218–3229. doi:10.4049/jimmunol.2000511

Reis, E. S., Mastellos, D. C., Ricklin, D., Mantovani, A., and Lambris, J. D. (2018). Complement in cancer: untangling an intricate relationship. *Nat. Rev. Immunol.* 18, 5–18. doi:10.1038/nri.2017.97

Riihilä, P., Nissinen, L., Knuutila, J., Rahmati Nezhad, P., Viiklepp, K., and Kähäri, V. M. (2019). Complement system in cutaneous squamous cell carcinoma. *Int. J. Mol. Sci.* 20, 3550. doi:10.3390/ijms20143550

Ruiz-Molina, N., Parsons, J., Decker, E. L., and Reski, R. (2023). Structural modelling of human complement FHR1 and two of its synthetic derivatives provides insight into their *in-vivo* functions. *Comput. Struct. Biotechnol. J.* 21, 1473–1486. doi:10.1016/j.csbj.2023.02.002

Saito, K., Arai, E., Maekawa, K., Ishikawa, M., Fujimoto, H., Taguchi, R., et al. (2016). Lipidomic signatures and associated transcriptomic profiles of clear cell renal cell carcinoma. *Sci. Rep.* 6, 28932. doi:10.1038/srep28932

Satariano, M., Ghose, S., and Raina, R. (2024). The pathophysiology of inherited renal cystic diseases. *Genes* 15, 91. doi:10.3390/genes15010091

Schneider, G., Bryndza, E., Poniewierska-Baran, A., Serwin, K., Suszynska, M., Sellers, Z. P., et al. (2016). Evidence that vitronectin is a potent migration-enhancing factor for cancer cells chaperoned by fibrinogen: a novel view of the metastasis of cancer cells to low-fibrinogen lymphatics and body cavities. *Oncotarget* 7, 69829–69843. doi:10.18632/oncotarget.12003

SciPy (2024a). scipy.stats.false_discovery_control — SciPy v1.13.0 Manual. Available at: https://docs.scipy.org/doc/scipy/reference/generated/scipy.stats.false_discovery_control.html.

SciPy (2024b). scipy.stats.mannwhitneyu — SciPy v1.13.0 Manual. Available at: https://docs.scipy.org/doc/scipy/reference/generated/scipy.stats.mannwhitneyu.html.

Selby, P. J., Banks, R. E., Gregory, W., Hewison, J., Rosenberg, W., Altman, D. G., et al.(2018). "Review and prioritisation of circulating biomarkers in renal cancer and renal transplantation," in *Methods for the evaluation of biomarkers in patients with kidney and liver diseases: multicentre research programme including ELUCIDATE RCT* (Southampton, UK: NIHR Journals Library). Available at: http://www.ncbi.nlm.nih.gov/books/NBK513103/ (Accessed December 19, 2024).

Shastri, S., Patel, J., Sambandam, K. K., and Lederer, E. D. (2023). Kidney stone pathophysiology, evaluation and management: core curriculum 2023. *Am. J. Kidney Dis.* 82, 617–634. doi:10.1053/j.ajkd.2023.03.017

Shen, X., Chen, Y., Zhang, Y., Xia, K., Chen, Y., and Hao, Z. (2022). The association of urine creatinine with kidney stone prevalence in US adults: data from NHANES 2009–2018. *Front. Med.* 9, 819738. doi:10.3389/fmed.2022.819738

Shoag, J., and Eisner, B. H. (2014). Relationship between C-reactive protein and kidney stone prevalence. *J. Urol.* 191, 372–375. doi:10.1016/j.juro.2013.09.033

Shuch, B., and Zhang, J. (2018). Genetic predisposition to renal cell carcinoma: implications for counseling, testing, screening, and management. *J. Clin. Oncol.* 36, 3560–3566. doi:10.1200/jco.2018.79.2523

Sindhughosa, D. A., and Pranamartha, A. G. M. K. (2017). The involvement of proinflammatory cytokines in diabetic nephropathy: focus on interleukin 1 (IL-1), interleukin 6 (IL-6), and tumor necrosis factor-alpha (TNF-α) signaling mechanism. *Bali Med. J.* 6, 44. doi:10.15562/bmj.v6i1.299

Singh, P., Harris, P. C., Sas, D. J., and Lieske, J. C. (2022). The genetics of kidney stone disease and nephrocalcinosis. *Nat. Rev. Nephrol.* 18, 224–240. doi:10.1038/s41581-021-00513-4

Sousa, M. V., Amaral, A. G., Freitas, J. A., Murata, G. M., Watanabe, E. H., Balbo, B. E., et al. (2021). Smoking accelerates renal cystic disease and worsens cardiac phenotype in Pkd1-deficient mice. *Sci. Rep.* 11, 14443. doi:10.1038/s41598-021-93633-7

sPLSDA SRBCT Case Study (2024). sPLSDA SRBCT Case Study | mixOmics. Available at: http://mixomics.org/case-studies/splsda-srbct-case-study/.

Stanford, S. M., and Bottini, N. (2023). Targeting protein phosphatases in cancer immunotherapy and autoimmune disorders. *Nat. Rev. Drug Discov.* 22, 273–294. doi:10.1038/s41573-022-00618-w

Stebbing, J., Lit, L. C., Zhang, H., Darrington, R. S., Melaiu, O., Rudraraju, B., et al. (2014). The regulatory roles of phosphatases in cancer. *Oncogene* 33, 939–953. doi:10.1038/onc.2013.80

Stepanov, A. A., Malsagova, K. A., Kopylov, A. T., Rudnev, V. R., Karateev, D. E., Markelova, E. I., et al. (2023). Determination of heterogeneous proteomic and metabolomic response in anti-TNF and anti-IL-6 treatment of patients with rheumatoid arthritis. *Life* 13, 596. doi:10.3390/life13020596

Sun, H., Samarghandi, A., Zhang, N., Yao, Z., Xiong, M., and Teng, B. B. (2012). Proprotein convertase subtilisin/kexin type 9 interacts with apolipoprotein B and prevents its intracellular degradation, irrespective of the low-density lipoprotein receptor. *Arterioscler. Thromb. Vasc. Biol.* 32, 1585–1595. doi:10.1161/ATVBAHA.112.250043

Sun, Y., Chen, H. J., Han, R. J., Zhao, C., Si, Y. Y., Li, M., et al. (2021). Causal associations between serum urea and cancer: a mendelian randomization study. *Genes* 12, 498–508. doi:10.1039/d1ra07498a

Takeuchi, M., McDonald, J. S., Takahashi, N., Frank, I., Thompson, R. H., King, B. F., et al. (2021). Cancer prevalence and risk stratification in adults presenting with hematuria: a population-based cohort study. *Mayo Clin. Proc. Innov. Qual. Outcomes* 5, 308–319. doi:10.1016/j.mayocpiqo.2020.12.001

Tikhonov, D., Kulikova, L., Kopylov, A. T., Rudnev, V., Stepanov, A., Malsagova, K., et al. (2021). Proteomic and molecular dynamic investigations of PTM-induced structural fluctuations in breast and ovarian cancer. *Sci. Rep.* 11, 19318. doi:10.1038/s41598-021-98201-7

Truong, H., and Carlo, M. I.(2022). "Hereditary cancer and genetics in renal cell carcinoma," in *Urologic oncology: multidisciplinary care for patients*. Editors K. L. s. Stratton, and A. K. Morgans (Cham: Springer International Publishing), 285–298. doi:10.1007/978-3-030-89891-5_14

Tseng, C.-H. (2015). Type 2 diabetes mellitus and kidney cancer risk: a retrospective cohort analysis of the national Health insurance. *PLoS ONE* 10, e0142480. doi:10.1371/journal.pone.0142480

Tung, H.-T., Liu, C.-M., Huang, H.-S., Lu, Z.-H., and Liu, C.-J. (2024). Author Correction: increased risk of chronic kidney disease in uric acid stone formers with high neutrophil-to-lymphocyte ratio. *Sci. Rep.* 14, 2096. doi:10.1038/s41598-024-52552-z

Tupikowski, K., Jaobsche-Policht, U., Bittner, J., Ptaszkowski, K., Halon, A., Zdrojowy, R., et al. (2023). The influences of selected clotting and fibrinolysis factors on survival of patients with kidney tumors - a prospective study. *Arch. Med. Sci. AMS* 19, 1003–1010. doi:10.5114/aoms/128845

Vakiti, A., Anastasopoulou, C., and Mewawalla, P.(2024). "Malignancy-related hypercalcemia," in *StatPearls* (Treasure Island (FL): StatPearls Publishing).

Vandooren, J., and Itoh, Y. (2021a). Alpha-2-Macroglobulin in inflammation, immunity and infections. *Front. Immunol.* 12, 803244. doi:10.3389/fimmu.2021.803244

Vandooren, J., and Itoh, Y. (2021b). Alpha-2-Macroglobulin in inflammation, immunity and infections. *Front. Immunol.* 12, 803244. doi:10.3389/fimmu.2021.803244

Vitale, C., Croppi, E., and Marangella, M. (2008). Biochemical evaluation in renal stone disease. *Clin. Cases Min. Bone Metab.* 5, 127–130.

Vivarelli, M., Barratt, J., Beck, L. H., Jr, Fakhouri, F., Gale, D. P., Goicoechea de Jorge, E., et al. (2024). The role of complement in kidney disease: conclusions from a kidney disease: improving global outcomes (KDIGO) controversies conference. *Kidney Int.* 106, 369–391. doi:10.1016/j.kint.2024.05.015

Walsh, M. T., Iqbal, J., Josekutty, J., Soh, J., Di Leo, E., Özaydin, E., et al. (2015). Novel abetalipoproteinemia missense mutation highlights the importance of the N-terminal

β-barrel in microsomal triglyceride transfer protein function. *Circ. Cardiovasc. Genet.* 8, 677–687. doi:10.1161/CIRCGENETICS.115.001106

Wang, X., Shi, A., Huang, J., Chen, Y., Xue, W., and Zhang, J. (2020). Assessment of hypercoagulability using thromboelastography predicts advanced status in renal cell carcinoma. *J. Clin. Lab. Anal.* 34, e23017. doi:10.1002/jcla.23017

Wei, L., Xiao, Y., Xiong, X., Li, L., Yang, Y., Han, Y., et al. (2020). The relationship between simple renal cysts and renal function in patients with type 2 diabetes. *Front. Physiol.* 11, 616167. doi:10.3389/fphys.2020.616167

Wigner, P., Grębowski, R., Bijak, M., Szemraj, J., and Saluk-Bijak, J. (2021). The molecular aspect of nephrolithiasis development. *Cells* 10, 1926. doi:10.3390/cells10081926

Wu, G., Wang, Q., Xu, Y., Li, J., Zhang, H., Qi, G., et al. (2019). Targeting the transcription factor receptor LXR to treat clear cell renal cell carcinoma: agonist or inverse agonist? *Cell Death Dis.* 10, 416. doi:10.1038/s41419-019-1654-6

Wu, G., Zhang, Z., Tang, Q., Liu, L., Liu, W., Li, Q., et al. (2020). Study of FABP's interactome and detecting new molecular targets in clear cell renal cell carcinoma. *J. Cell. Physiol.* 235, 3776–3789. doi:10.1002/jcp.29272

Wu, Y., Lu, C., Pan, N., Zhang, M., An, Y., Xu, M., et al. (2021). Serum lactate dehydrogenase activities as systems biomarkers for 48 types of human diseases. *Sci. Rep.* 11, 12997. doi:10.1038/s41598-021-92430-6

Xi, W., Liu, L., Wang, J., Xia, Y., Bai, Q., Long, Q., et al. (2016). High level of anaphylatoxin C5a predicts poor clinical outcome in patients with clear cell renal cell carcinoma. *Sci. Rep.* 6, 29177. doi:10.1038/srep29177

Xiao, J., Zheng, S., Qiu, Z., and Wu, K. (2022). Associations between *IL-1RN* variable number of tandem repeat, *IL-1β* (-511) and *IL-1β* (+3954) gene polymorphisms and urolithiasis in Uighur children of China. *Asian J. Urol.* 9, 51–56. doi:10.1016/j.ajur.2021.04.009

Xiao, X., Zhang, J., Lang, Y., Cai, L., Yang, Q., Liu, K., et al. (2023). Associations of lactate dehydrogenase with risk of renal outcomes and cardiovascular mortality

in individuals with diabetic kidney disease. *Diabetes Res. Clin. Pract.* 203, 110838. doi:10.1016/j.diabres.2023.110838

Yang, B., Fu, L., Privratsky, J. R., Lu, X., Ren, J., Mei, C., et al. (2019). Interleukin-1 receptor activation aggravates autosomal dominant polycystic kidney disease by modulating regulated necrosis. *Am. J. Physiol. - Ren. Physiol.* 317, F221–F228. doi:10.1152/ajprenal.00104.2019

Yang, H., Sieben, C. J., Schauer, R. S., and Harris, P. C. (2023). Genetic spectrum of polycystic kidney and liver diseases and the resulting phenotypes. *Adv. Kidney Dis. Health* 30, 397–406. doi:10.1053/j.akdh.2023.04.004

Yanus, G. A., Kuligina, E. S., and Imyanitov, E. N. (2024). Hereditary renal cancer syndromes. *Med. Sci.* 12, 12. doi:10.3390/medsci12010012

Yu, Y., Ma, L., Wang, Z., and Zhang, Z. (2017). Renal cell carcinoma presenting as a simple renal cyst: a case report. *Mol. Clin. Oncol.* 6, 550–552. doi:10.3892/mco.2017.1173

Zhang, J., Zamani, M., Thiele, C., Taher, J., Amir Alipour, M., Yao, Z., et al. (2017a). AUP1 (ancient ubiquitous protein 1) is a key determinant of hepatic very-low-density lipoprotein assembly and secretion. *Arterioscler. Thromb. Vasc. Biol.* 37, 633–642. doi:10.1161/ATVBAHA.117.309000

Zhang, L., and Bu, P. (2022). The two sides of creatine in cancer. *Trends Cell Biol.* 32, 380–390. doi:10.1016/j.tcb.2021.11.004

Zhang, X., Saarinen, A. M., Hitosugi, T., Wang, Z., Wang, L., Ho, T. H., et al. (2017b). Inhibition of intracellular lipolysis promotes human cancer cell adaptation to hypoxia. *eLife* 6, e31132. doi:10.7554/eLife.31132

Zhou, L., Cai, X., Liu, Q., Jian, Z. Y., Li, H., and Wang, K. J. (2015). Prognostic role of C-reactive protein in urological cancers: a meta-analysis. *Sci. Rep.* 5, 12733. doi:10.1038/srep12733

Zhu, Z., Liu, M., Zhang, Y., Wu, J., Gao, M., Lei, T., et al. (2023). Risk factors for the comorbidity of osteoporosis/osteopenia and kidney stones: a cross-sectional study. *Arch. Osteoporos.* 18, 128. doi:10.1007/s11657-023-01338-3